REVIEW ARTICLE

Structural analyses reveal two distinct families of nucleoside phosphorylases

Matthew J. PUGMIRE and Steven E. EALICK[1]

Department of Chemistry and Chemical Biology, Cornell University, Ithaca, NY 14853, U.S.A.

The reversible phosphorolysis of purine and pyrimidine nucleosides is an important biochemical reaction in the salvage pathway, which provides an alternative to the *de novo* purine and pyrimidine biosynthetic pathways. Structural studies in our laboratory and by others have revealed that only two folds exist that catalyse the phosphorolysis of all nucleosides, and provide the basis for defining two families of nucleoside phosphorylases. The first family (nucleoside phosphorylase-I) includes enzymes that share a common single-domain subunit, with either a trimeric or a hexameric quaternary structure, and accept a range of both purine and pyrimidine nucleoside substrates. Despite differences in substrate specificity, amino acid sequence and quaternary structure, all members of this family share a characteristic subunit topology. We have also carried out a sequence motif study that identified regions of the common subunit fold that are functionally significant in differentiating the various members of the nucleoside phosphorylase-I family. Although the substrate-binding sites are arranged similarly for all members of the nucleoside phosphorylase-I family, a comparison of the active sites from the known structures of this family indicates significant differences between the trimeric and hexameric family members. Sequence comparisons also suggest structural identity between the nucleoside phosphorylase-I family and both 5′-methylthioadenosine/*S*-adenosylhomocysteine nucleosidase and AMP nucleosidase. Members of the second family of nucleoside phosphorylases (nucleoside phosphorylase-II) share a common two-domain subunit fold and a dimeric quaternary structure, share a significant level of sequence identity ($> 30\,\%$) and are specific for pyrimidine nucleosides. Members of this second family accept both thymidine and uridine substrates in lower organisms, but are specific for thymidine in mammals and other higher organisms. A possible relationship between nucleoside phosphorylase-II and anthranilate phosphoribosyltransferase has been identified through sequence comparisons. Initial studies in our laboratory suggested that members of the nucleoside phosphorylase-II family require significant domain movements in order for catalysis to proceed. A series of recent structures has confirmed our hypothesis and provided details of these conformational changes. Structural studies of the nucleoside phosphorylases have resulted in a wealth of information that begins to address fundamental biological questions, such as how Nature makes use of the intricate relationships between structure and function, and how biological processes have evolved over time. In addition, the therapeutic potential of suppressing the nucleoside phosphorylase activity in either family of enzymes has motivated efforts to design potent inhibitors. Several research groups have synthesized a variety of nucleoside phosphorylase inhibitors that are at various stages of preclinical and clinical evaluation.

Key words: active site, inhibitors, purine nucleoside phosphorylase, pyrimidine nucleoside phosphorylase, quaternary structure.

INTRODUCTION TO THE NUCLEOSIDE PHOSPHORYLASES

Biochemical processes involving nucleotides and nucleotide precursors are some of the most ubiquitous and fundamental in the function and survival of the cell. One such biochemical reaction that has been studied for many years is the phosphorolysis of purine and pyrimidine nucleosides, whereby the C–N glycosidic bond is cleaved by a phosphate ion to yield the free base and ribose 1-phosphate. The enzymic cleavage of the glycosidic bond in purine and pyrimidine ribosides was first noted by Levene [1], even before the detailed structure of nucleic acids was fully understood. The discovery of the enzyme responsible for this cleavage has been attributed to Levene and Medigreceanu [2]. Later, in 1924, Levene and co-workers published two papers on the general properties [3] and purification methods [4] of nucleosidase, as the enzyme had come to be called. Additional studies confirmed the enzymic cleavage of the glycosidic bonds in pyrimidines [5,6] and demonstrated the existence of two separate types of nucleosidases: one specific for purines and another specific for pyrimidines. Earlier work [2] had suggested, however, that no phosphorylase cleaves the glycosidic bond of cytidine. Details of the glycosidic cleavage were enhanced in 1945 when Kalckar showed the second product of the reaction to be ribose 1-phosphate [7,8] instead of ribose, as had been previously supposed. This new evidence gave rise to the idea that the glycosidic cleavage was due to a phosphorolysis reaction, rather than hydrolysis, where P_i attacks the ribose at the C-1′ position. The proposed enzymic reaction for the purine nucleosides was then established as:

$$\text{Purine nucleoside} + \text{phosphate} \leftrightarrow \text{ribose 1-phosphate} + \text{purine base}$$

Further work by Kalckar [9] confirmed this mechanism for the purine nucleoside phosphorylase (PNP), and further suggested that this reversible phosphorolysis is likely to be ''a reaction of wide significance''. Kalckar [9] also suggested that the same

Abbreviations used: AnPRT, anthranilate phosphoribosyltransferase; MTA/SAH, 5′-methylthioadenosine/*S*-adenosylhomocysteine; MTAP, 5′-deoxy-5′-methylthioadenosine phosphorylase; hMTAP, human MTAP; NP-I, nucleoside phosphorylase-I; NP-II, nucleoside phosphorylase-II; PNP, purine nucleoside phosphorylase; bPNP, bovine PNP; hPNP, human PNP; PyNP, pyrimidine nucleoside phosphorylase; TP, thymidine phosphorylase; UP, uridine phosphorylase.

[1] To whom correspondence should be addressed (e-mail see3@cornell.edu).

mechanism is involved in catalysis by pyrimidine nucleoside phosphorylase (PyNP):

Pyrimidine nucleoside + phosphate ↔ ribose 1-phosphate + pyrimidine base

Studies characterizing the general properties and purification methods of PyNP from horse liver appeared in 1954 [10,11], and showed that thymidine was cleaved but that uridine was not. This observation suggested the presence of two PyNPs: one specific for thymidine and one specific for uridine. This was supported by the earlier work of Paege and Schlenk [12], in which bacterial PyNP was shown to cleave uridine but not thymidine. This work also provided conclusive evidence for a reversible phosphorolytic mechanism for PyNP, analogous to the mechanism determined earlier for PNP.

In addition to phosphorolysis, other reactions for cleaving glycosidic bonds have now been identified. The C–N glycosidic bond is hydrolysed in nucleosides and dinucleotides by nucleoside hydrolases, which include examples such as inosinase (EC 3.2.2.2) [13], uridine nucleosidase (EC 3.2.2.3) [14], 5′-methylthioadenosine/*S*-adenosylhomocysteine (MTA/SAH) nucleosidase (EC 3.2.2.9) [15], AMP nucleosidase (EC 3.2.2.4) [16] and NAD^+ nucleosidase (EC 3.2.2.5) [17]. The glycoside hydrolase enzymes, which also have a hydrolytic mechanism, cleave the glycosidic linkage in a variety of glycosides, and include examples such as lysozyme (EC 3.2.1.17) [18], β-galactosidase (EC 3.2.1.23) [19] and neuraminidase (EC 3.2.1.18) [20]. Nucleoside deoxyribosyltransferases catalyse the transfer of purine or pyrimidine bases between nucleosides (e.g. EC 2.4.2.5 and EC 2.4.2.6) and utilize specific residues of the enzyme as the nucleophile in cleaving the glycosidic bond [21]. However, in the absence of a second acceptor base, 2′-deoxyribosyltransferase also shows a secondary hydrolytic mechanism [22]. The phosphoribosyltransferases utilize pyrophosphate in glycosidic bond cleavage, and include examples such as adenine phosphoribosyltransferase (EC 2.4.2.7) [23], hypoxanthine–guanine phosphoribosyltransferase (EC 2.4.2.8) [24], nicotinamide phosphoribosyltransferase (EC 2.4.2.11) [25] and anthranilate phosphoribosyltransferase (AnPRT; EC 2.4.2.18) [26].

The biochemical significance of glycosidic bond cleavage in purines and pyrimidines by the phosphorolytic mechanism catalysed by PNPs and PyNPs is most apparent in the salvage pathway [27,28]. The biosynthesis of purine and pyrimidine nucleotides, which are critical compounds in nearly all biochemical processes, can proceed through one of two pathways in the cell: (1) the *de novo* pathway, which uses a variety of amino acids and other low-level precursors to produce nucleotides, and (2) the salvage pathway, which makes use of preformed nucleobases and nucleosides as precursors in the production of nucleotides. The salvage pathway thus allows the cell to circumvent the energy-costly *de novo* pathway when appropriate precursors are available. In addition, the side products released in the salvage pathway provide a source of carbon, nitrogen and energy (via the conversion of the ribose moiety into intermediates that can enter the pentose phosphate pathway and glycolysis) to the cell. In addition to its role in the salvage pathway, thymidine phosphorylase (TP) has also been shown to have deoxyribosyltransferase activity, which results in the deoxyribosyl moiety being transferred from one base to another. This transferase activity is also known to play an important role in the metabolism of nucleosides [29].

Biomedical interest in the nucleoside phosphorylases arises from their key role in nucleotide metabolism and their requirement for normal cellular function. Nucleoside phosphorylases affect the cellular levels of free bases and nucleosides by catalysing their interconversion. It has been suggested that inhibitors of specific nucleoside phosphorylases might potentiate the action of certain nucleoside analogues of chemotherapeutic value by preventing their cleavage and subsequent inactivation [30]. PNP is required for normal T-cell development. Patients lacking PNP have severe T-cell immune deficiency, while B-cell function is unaffected [31]. This clinical profile suggests that inhibitors of human PNP (hPNP) might be used to selectively kill T-cells in T-cell leukaemias and T-cell lymphomas, to suppress the T-cell response after organ transplantation, or to treat T-cell-mediated autoimmune diseases [32]. Mammalian TP is associated with angiogenesis. Originally identified as platelet-derived endothelial cell growth factor [33], TP is now the target of a number of groups seeking to develop inhibitors for the treatment of metastatic tumours.

PNP from *Escherichia coli* is also of biomedical interest because of the potential to develop cancer treatments that utilize gene therapy to activate nucleoside analogues to their cytotoxic form [34]. In particular, tumour cells transfected with the *E. coli* PNP gene are able to cleave non-toxic prodrugs such as 6-methylpurine-2′-deoxyribose to the highly cytotoxic base 6-methylpurine [35]. Furthermore, the liberated 6-methylpurine can pass through the cell membrane and kill nearby cells through a 'bystander' effect. The prodrug is not cleaved by hPNP because of significant differences in substrate specificity between the bacterial and mammalian enzymes. Finally, the nucleoside phosphorylases of some micro-organisms are potential therapeutic targets. Because of the differences in substrate specificity between hPNP and PNPs from micro-organisms [36], it may be possible to selectively inhibit purine salvage. This might be particularly advantageous in parasitic organisms that lack *de novo* synthesis and rely entirely on the salvage pathway as a source of purines.

Because of the recent emphasis on functional genomics, and because structure is more highly conserved than sequence, it is becoming ever more important to relate protein structure to protein function. Over the last few years we have shown, using structural studies, that all of the enzymes that catalyse the phosphorolytic cleavage of the glycosidic bond in nucleosides have one of two distinct protein folds. This is the case even though these enzymes show a wide range of substrate specificities and physical properties, and in many cases low sequence identity. The discovery of only two possible folds provides the basis for our definition of two distinct families of nucleoside phosphorylases. Here we define the nucleoside phosphorylase-I (NP-I) family as those enzymes that share a common α/β-subunit fold and show either a trimeric or a hexameric quaternary structure. Members of the NP-I family accept a range of purine nucleosides, as well as the pyrimidine nucleoside uridine. Furthermore, we define the nucleoside phosphorylase-II (NP-II) family to be those enzymes that display a dimeric quaternary structure where each characteristic subunit consists of a small α-domain separated by a large cleft from a larger α/β-domain. Members of the NP-II family accept both thymidine and uridine in lower organisms, but are specific for thymidine in higher species, including humans. The discovery of two distinct protein folds that catalyse the same fundamental biochemical reaction provides a unique example of how Nature makes use of structural diversity to accomplish a common task.

NP-I FAMILY

PNP is perhaps the most thoroughly studied member of the NP-I family. Since the early work by Kalckar [9] in which PNP (EC 2.4.2.1) was originally classified, this enzyme has been isolated

and studied from a variety of species. Kalckar [37] was among the first to successfully isolate PNP when he purified the enzyme from rat liver tissue. Later, Kim and co-workers [38] successfully purified and partially characterized PNP from human erythrocytes. PNP has now been isolated and studied from a wide variety of both mammalian (e.g. bovine brain [39], rabbit liver [40], calf spleen [41] and hamster [42]) and bacterial (e.g. *E. coli* and *Salmonella typhimurium* [43], *Sulfolobus solfataricus* [44], *Erwinia carotovora* [45] and *Bacillus cereus* T [46]) species. These studies have revealed two forms of PNP: (1) trimeric PNP, which has a subunit molecular mass of approx. 31 kDa and is specific for guanine and hypoxanthine (2′-deoxy)ribonucleosides; and (2) hexameric PNP, which has a subunit molecular mass of approx. 26 kDa and accepts adenine as well as guanine and hypoxanthine (2′-deoxy)ribonucleosides. Mammalian species generally possess only the trimeric form of PNP. Bacterial species have largely been shown to possess only the hexameric form, although both a trimeric and a hexameric form have been found in *E. coli* [47], *Bacillus subtilis* [48] and *Bacillus stearothermophilus* [49].

Other members of the NP-I family include uridine phosphorylase (UP; EC 2.4.2.3) and 5′-deoxy-5′-methylthioadenosine phosphorylase (MTAP; EC 2.4.2.28). UP, which is specific for uridine nucleosides, but also accepts 2′-deoxypyrimidine nucleosides in higher organisms [50], has been isolated and characterized from a variety of species [51–54]. Bacterial UP functions as a hexamer with identical subunits that have a molecular mass most commonly reported as 27.5 kDa. A study of UP from a variety of organisms by Krenitsky and co-workers [50] showed two distinct types of UP, as distinguished by pH optima at either 6.5–6.7 or 7.9–8.1. MTAP, which is specific for the purine nucleoside analogue 5′-deoxy-5′-methylthioadenosine, has been isolated and characterized from bacterial and mammalian species [44,55,56]. MTAP is reported to function as a trimer in all species with the exception of *Sulfolobus solfataricus* [44], in which it reportedly functions as a hexamer. MTAP consists of identical subunits each with a molecular mass of approx. 30 kDa, except in the archaeal enzyme, which has a slightly smaller subunit.

Although nucleoside synthesis is favoured thermodynamically, phosphorolysis generally occurs *in vivo* due to the uptake of the free bases as reactants in subsequent reactions [30,57]. Several different mechanisms for the phosphorolysis reaction have been suggested for members of the NP-I family from different species. Early kinetic data from human erythrocyte and bovine spleen PNPs indicated that catalysis occurs through a ternary complex of enzyme, phosphate and nucleoside, and that the reaction is sequential rather than Ping Pong [58,59]. Studies with PNP from bovine thyroid indicated an ordered Bi Bi mechanism, with phosphate binding before the nucleoside [60], while the reverse order has been reported for the enzyme from bovine brain [39]. A Theorell–Chance mechanism has also been reported for PNP in human erythrocytes [61]. A more recent study reported kinetic data from bovine spleen PNP that are consistent with an ordered-sequential mechanism in the phosphorolytic direction, with phosphate binding before the nucleoside, and a random-sequential mechanism in the synthetic direction [62]. Studies based on site-directed mutagenesis, X-ray structures and kinetic data have provided a detailed model for the proposed transition state of PNP [63–65]. Further studies of the structural mechanisms of *Cellulomonas* and bovine PNPs suggested a primary role for water in stabilizing the transition state [66,67]. Kinetic studies of UP from different species have reported both a random-sequential mechanism [52] and an ordered-sequential mechanism in which phosphate is the first substrate to bind and uracil is the first product to leave [68]. Kinetic studies on MTAP have similarly reported both a random-sequential mechanism [69] and an ordered-sequential mechanism in which 5′-deoxy-5′-methylthioadenosine is the first substrate to bind and 5′-methylthioribose 1-phosphate is the first product to leave [70,71].

NP-I STRUCTURES

X-ray crystallographic studies in our laboratory and others have now provided several crystal structures of members of the NP-I family in both native and complex forms. The PNP fold was first revealed in studies on the crystal structure of trimeric human erythrocyte PNP (hPNP) in which the native enzyme, as well as complexes with the substrate analogues 8-iodoguanine and 5′-iodoformycin B, were solved at 3.2 Å resolution [72]. The complex with guanine was also reported [32], and the refinement of the native enzyme was extended to 2.75 Å [73], the limit of diffraction of the crystals. The structure of PNP from calf spleen (bovine PNP; bPNP) was first reported at 2.9 Å [74], and has more recently been reported at higher resolution ($\approx$ 2 Å) in both native and complex forms [75,76]. Most recently, structures of bPNP have been reported for complexes with acycloguanine [77] and with immucillin, a transition-state analogue [66]. Other trimeric PNP structures include those of *Cellulomonas* sp. PNP [67] and PNP from *Mycobacterium tuberculosis* [78]. The first structure of human MTAP (hMTAP) was solved at 1.7 Å [79], and the enzyme was shown to be homologous with the trimeric PNPs. Structures of hexameric PNP have been reported for the enzyme from *E. coli* at 2.0 Å [80] and at 2.1 Å [81] resolution. The structure of UP from *E. coli* was first reported at 3.0 Å [82], and then later at 2.5 Å [83]. Most recently, the structure of a hexameric MTAP from *Sulfolobus solfataricus* was determined [84]. This enzyme is similar to *E. coli* PNP and also catalyses the phosphorolysis of inosine, guanosine and adenosine; however, *E. coli* PNP is unable to cleave methylthioadenosine.

Despite species-dependent differences in the quaternary structures of members of the NP-I family (Figure 1a), the subunit fold is highly conserved. Topology diagrams that are representative of the subunit folds from both the trimeric and hexameric assemblies are shown in Figure 1(b). The main feature of the common subunit fold of NP-I enzymes consists of a central β-sheet that forms a distorted β-barrel, surrounded by several α-helices (Figure 1c). hMTAP shows a trimeric quaternary structure very similar to that seen in mammalian PNP, while the structure of *E. coli* UP reveals a hexameric quaternary structure that is very similar to that of *E. coli* PNP. The active site in members of the NP-I family consists of adjacent phosphate- and nucleoside-binding pockets. These binding sites are formed by residues from the central β-sheet and the interconnecting loops, and residues from an adjacent subunit. Superimposing representative structures of NP-I reveals that four of the α-helices (H3, H4, H6 and H7, using bPNP numbering as a reference), as well as 12 of the β-strands (A1–A8, 1B, 2B, 3B and 5B), are structurally conserved (Figure 2). Other structurally conserved regions include H5 and 4B among bPNP, hPNP and hMTAP, and H1 and H2 among bPNP and hPNP.

It is significant that, with the exception of strand 4B, all of the β-strands are structurally conserved among the structures of the NP-I family. This central β-sheet structural motif, where the nucleoside and phosphate bind at the C-terminal end of the strands, is completely conserved, despite divergence in the sequences among the structures (see below). This suggests a structural motif that is important in binding nucleosides and phosphate and in catalysing the phosphorolysis reaction. Members of the GTPase family bind nucleotides and also incorporate a central β-sheet topology that is similar to that seen

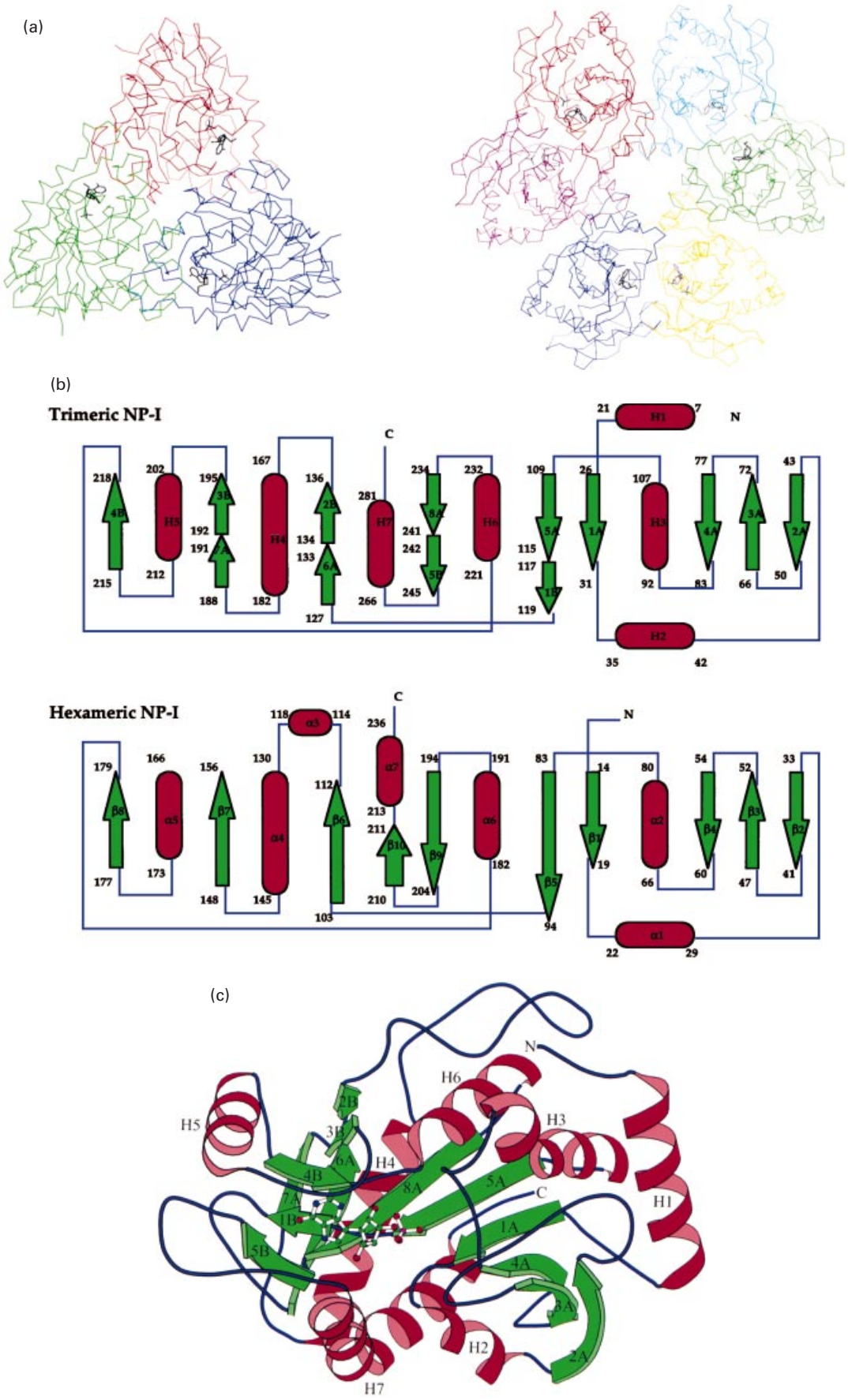

Figure 1 For legend see opposite

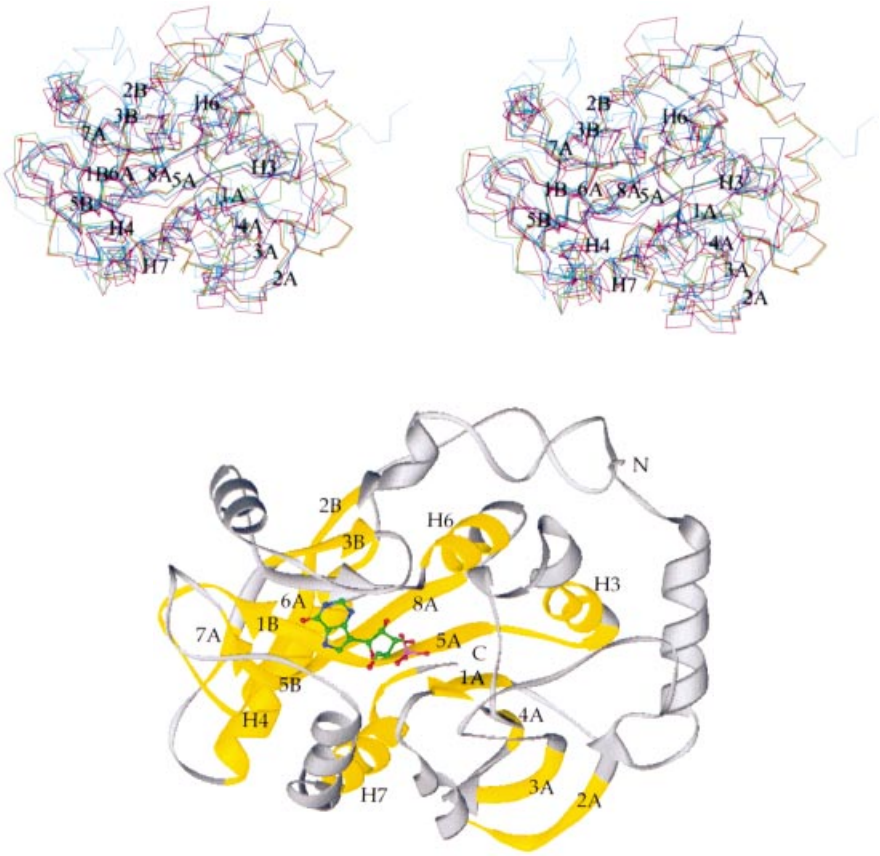

Figure 2 Structural conservation in the NP-I family

Upper panel: stereoview of the Cα traces of structures of the NP-I family following superposition. The five models are coloured: red, bPNP; green, erythrocyte hPNP; blue, hMTAP; violet, *E. coli* PNP; cyan, *E. coli* UP. This Figure was produced using MOLSCRIPT [162]. Lower panel: ribbon drawing of a subunit of bPNP in which the regions that are structurally conserved between all members of the NP-I family have been coloured yellow and labelled. This Figure was produced with RIBBONS [163].

in the C-terminal half of structures of the NP-I family. The conserved helices are also likely to play an important role in the structure–function relationship of the NP-I family. The four conserved helices are distributed on both sides of the central β-sheet and contribute to the overall stability of the α/β-fold. In addition, the N-terminal region of H6 contributes active-site residues to the phosphate-binding site. The most highly conserved region in the structures of NP-I members is the region including the loop between β-strands 5A and 1B, and between 1B and 6A. This loop region connects β-sheets A and B and contributes a residue (Ala-116 in bPNP) to the phosphate-binding pocket.

NP-I SEQUENCE COMPARISONS

The sequences of all known members of the NP-I family have been gathered from the protein databases using standard searching methods, and have not revealed any significant relationships with other protein families. Sequence comparisons of the known structures of NP-I enzymes alone suggest two NP-I subfamilies. There appears to be obvious identity among sequences with a known trimeric quaternary structure, and also among sequences with a known hexameric quaternary structure (Table 1). However, little sequence similarity is seen between the trimeric and hexameric NP-I subfamilies. Despite the lack of similarity between the trimeric and hexameric sequences, the structural similarity between the hexameric and trimeric monomers suggests a common ancestor. This subdivision in the NP-I family is also seen using the BLAST algorithm [85] to search the protein databases, where NP-I sequences fall into one of two groups: one subfamily shows greater similarity to the trimeric PNPs, while the other subfamily shows greater similarity to the hexameric PNPs. A sequence grouped in one NP-I subfamily does not

Figure 1 Structure and topology of NP-I enzymes

(**a**) Cα traces showing the trimeric and hexameric quaternary structures of the NP-I family. The representative trimeric structure (left) is that of bPNP, and the representative hexameric structure (right) is that of *E. coli* PNP. The active-site locations in each subunit are indicated by the substrate positions, which are drawn as stick models. The Figure was produced with MOLSCRIPT [162]. (**b**) Representative topologies from the trimeric and hexameric subfamilies of NP-I. The trimeric topology is that of bPNP (α-helices are shown as red cylinders and are labelled H1–H7; β-strands are shown as green arrows, where strands making up sheet A are labelled 1A–8A and those making up sheet B are labelled 1B–5B). The hexameric topology is that of *E. coli* PNP [α-helices (red) are labelled α1–α7, and β-strands (green) are labelled β1–β10]. The first and last residue numbers for each secondary structural element are listed. (**c**) Ribbon drawing of a subunit of bPNP in which the secondary structural elements have been labelled. The substrates are represented as ball-and-stick models to indicate the position of the active site. This Figure was produced with MOLSCRIPT [162].

Table 1 Sequence identity among structures of the NP-I family displaying trimeric (tri) or hexameric (hex) quaternary structure

	Identity (%)				
	hPNP (tri)	bPNP (tri)	MTAP (tri)	*E. coli* PNP (hex)	*E. coli* UP (hex)
hPNP (tri)	–	86.5	24.5	20.1	18.4
bPNP (tri)	86.5	–	25.5	19.4	17.9
MTAP (tri)	24.5	25.5	–	18.5	20.1
E. coli PNP (hex)	20.1	19.4	18.5	–	26.7
E. coli UP (hex)	18.4	17.9	20.1	26.7	–

detect a member of the other subfamily using standard searching methods. This sequence analysis has revealed that the trimeric subfamily can be divided further into PNP and MTAP sequences, while the hexameric subfamily can be divided further into PNPs, UPs and a set of uncharacterized hypothetical proteins. Multiple sequence alignments of each of these subfamilies are shown in Figure 3.

A motif analysis of all known sequences of the NP-I family has revealed interesting results that help to clarify what distinguishes a trimeric from a hexameric sequence [86]. Highly conserved regions of the sequences were determined using the MEME software [87], and examined with regard to their structural location. The analysis identified nine structural regions within the NP-I fold (Figure 4 and Table 2 below) where motifs were found. The structural regions are labelled A–I. The motifs for specific groups of enzymes are labelled A_j–I_j, where the subscript j indicates the group number for motifs that have different sequences but occur in the same structural region. The sequences that contain these motifs and their location in the primary sequence have been indicated in the multiple sequence alignments in Figure 3. The subfamily sequence specificity of each motif has also been indicated in Figure 4. Of the nine corresponding structural regions where the NP-I sequences are highly conserved, seven are involved in the active site, and six are involved in inter-subunit contacts. With the exception of motif A_1, which was found in all NP-I sequences, all of the motifs discovered were specific to either the trimeric or the hexameric subfamilies. The A_1 motif is important, since it is the only motif that is found in sequences from both the trimeric and hexameric subfamilies. The A_1 motif makes up the C-terminal end of β-strand 5A in bPNP, β-strand 1B, followed by a β-turn and the N-terminal portion of β-strand 6A. Comparing the structures of the NP-I family shows that there is a high degree of structural similarity in this region (see Figure 2). The structural conservation of this region is likely to be due to its proximity to and, consequently, its function in the active site. The beginning of this motif forms a portion of the phosphate-binding site (Ala-116 in bPNP), while the subsequent C-terminal portion of strand 1B and the subsequent loop, although not providing residues having direct contact with the purine base, nevertheless form the backside surface of the base-binding site. Mushegian and Koonin [88] found a similar motif in residues 111–134 of hPNP and in residues 85–108 of *E. coli* PNP. Sequence motifs that occur in corresponding structural regions where inter-subunit contacts are formed and appear to specify the trimeric quaternary structure include C_1, E_1 and G_1, while those that specify the hexameric quaternary structure include B_2, C_2, D_2, E_2 and F_2. It is likely that the highly conserved motifs in these regions are important in maintaining either the trimeric or the hexameric quaternary structure of the NP-I fold, and represent regions that differentiate members of the trimeric subfamily from members of the hexameric subfamily.

Several of the motifs occur in the active site of the NP-I fold. Active-site motifs that are only found in trimeric sequences include B_1, C_1, D_1, E_1, F_1 and H_1, while motifs in the active site of hexameric sequences include B_2, C_2, D_2 and E_2. It has been noted previously from structural comparisons of trimeric and hexameric PNPs that different modes of both phosphate and nucleoside binding exist [80]. Four motif regions involved in phosphate binding show specific motifs for the trimeric PNP sequences (B_1, D_1, E_1 and F_1) and for the hexameric PNP sequences (B_2, D_2 and E_2). A motif similar to B_2 has been reported previously [88] within residues 171–204 of *E. coli* PNP, although no structural or functional significance was noted. The E region is particularly interesting, since it contains residues that form a catalytic triad thought to be important in phosphate binding in bPNP, but which is not present in *E. coli* PNP. Mushegian and Koonin [88] speculated that a large motif in *E. coli* PNP (residues 48–77) is involved in phosphate binding. This motif corresponds to motifs E_2 and F_2 in our analysis. Similar to the motif regions that are involved in phosphate binding, there are two regions that are involved in nucleoside base binding that show specific motifs in the trimeric sequences (C_1 and H_1) and in the hexameric sequences (C_2 and H_3). These motifs are likely to play an important role in the differences in purine nucleoside specificity that exist between trimeric and hexameric forms of the NP-I family.

Two motifs (E_3 and H_2) have been found only in MTAP sequences, and may be distinguishing factors for MTAP function. It is significant that the loop region where E_3 occurs forms part of the binding site that is near the 5′ position of the ribose moiety wherein lies the specificity of the MTAP substrates. A unique sequence in this region may be important for the specificity of MTAP and would contribute to distinguishing it from PNP. Motif H occurs in β-strand 8A and part of the preceding loop, and contributes the active-site residue Asn-243 in bPNP. This residue is required both for catalysis and for conferring specificity for 6-oxo purine substrates. It is interesting that, in the case of MTAP, which binds the adenosine base and is thus specific for the 6-amino position, there is a unique sequence located in the functional region of this specificity. Due to the difference in substrate specificity between PNP and MTAP, it is perhaps not surprising that there are distinct motifs in the MTAP sequences that differentiate them from the general trimeric sequences of the NP-I family.

NP-I ACTIVE-SITE ANALYSIS

A structural comparison of the NP-I active sites provides a meaningful perspective concerning the relationships that exist in members of this family. While the phosphorolysis reaction is common to all enzymes of the NP-I family, there are significant differences in nucleoside specificities among the family members. Trimeric PNPs (e.g. bPNP and hPNP) are specific for 6-oxo

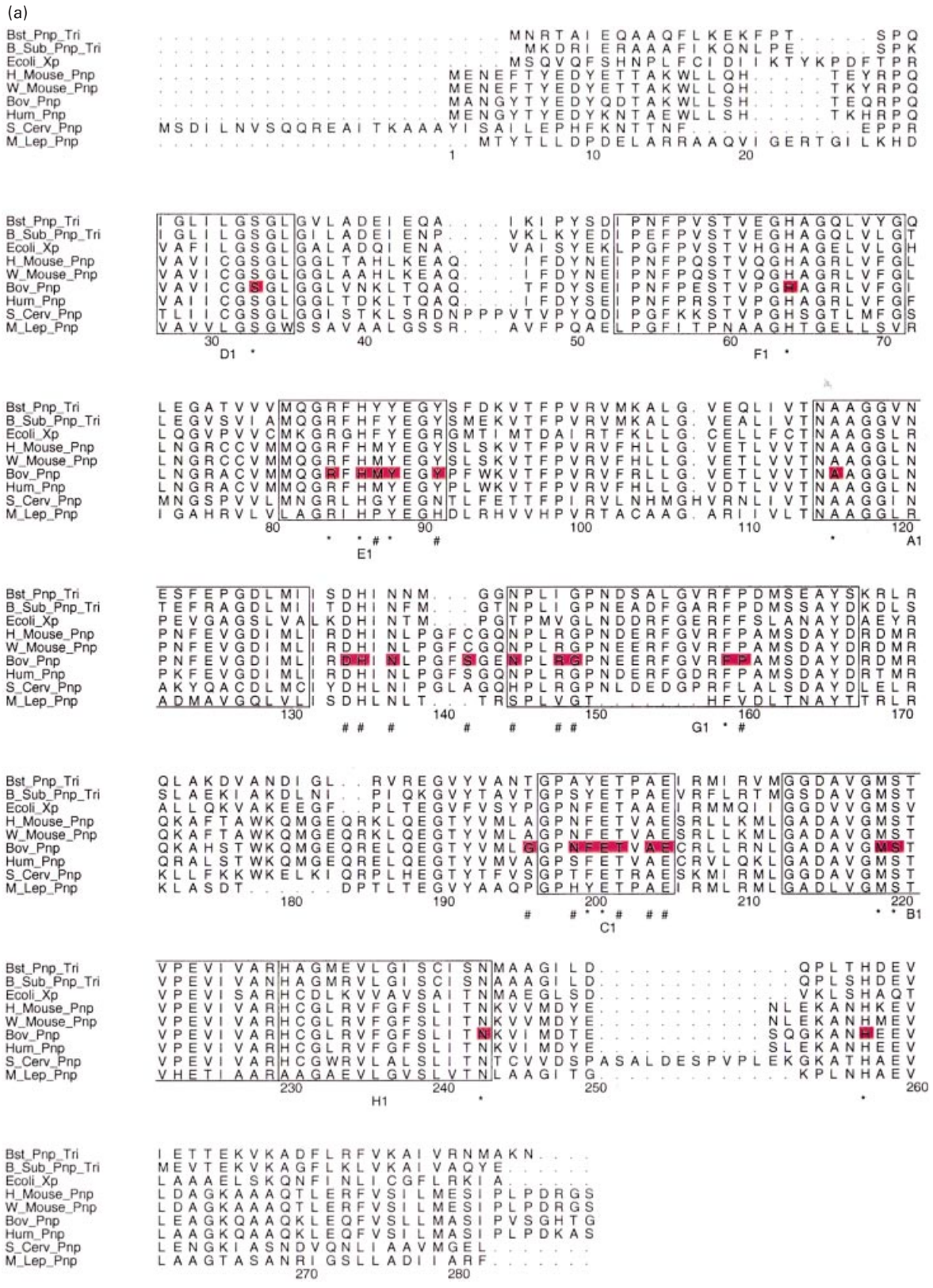

Figure 3 For legend see page 11

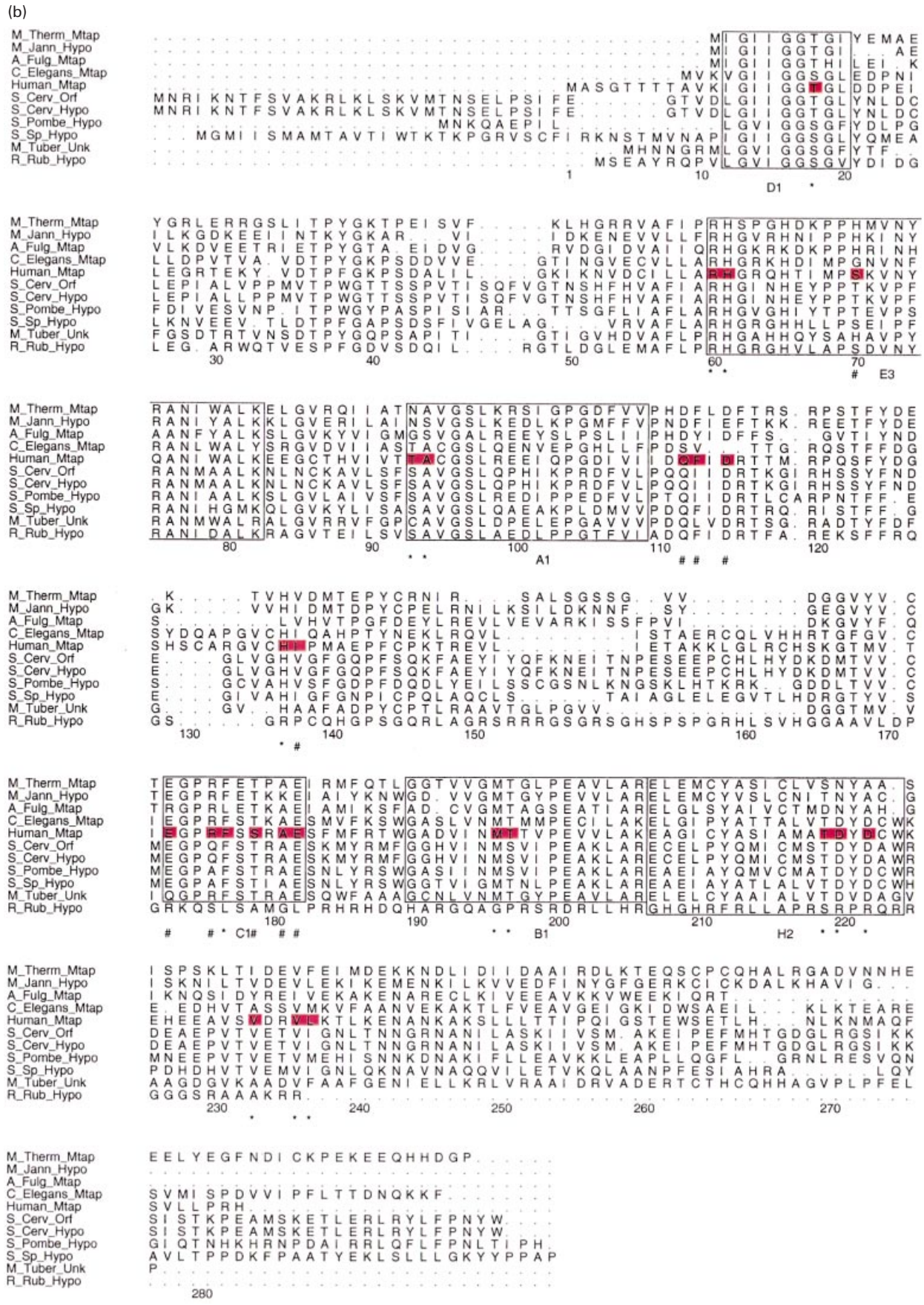

Figure 3 For legend see page 11

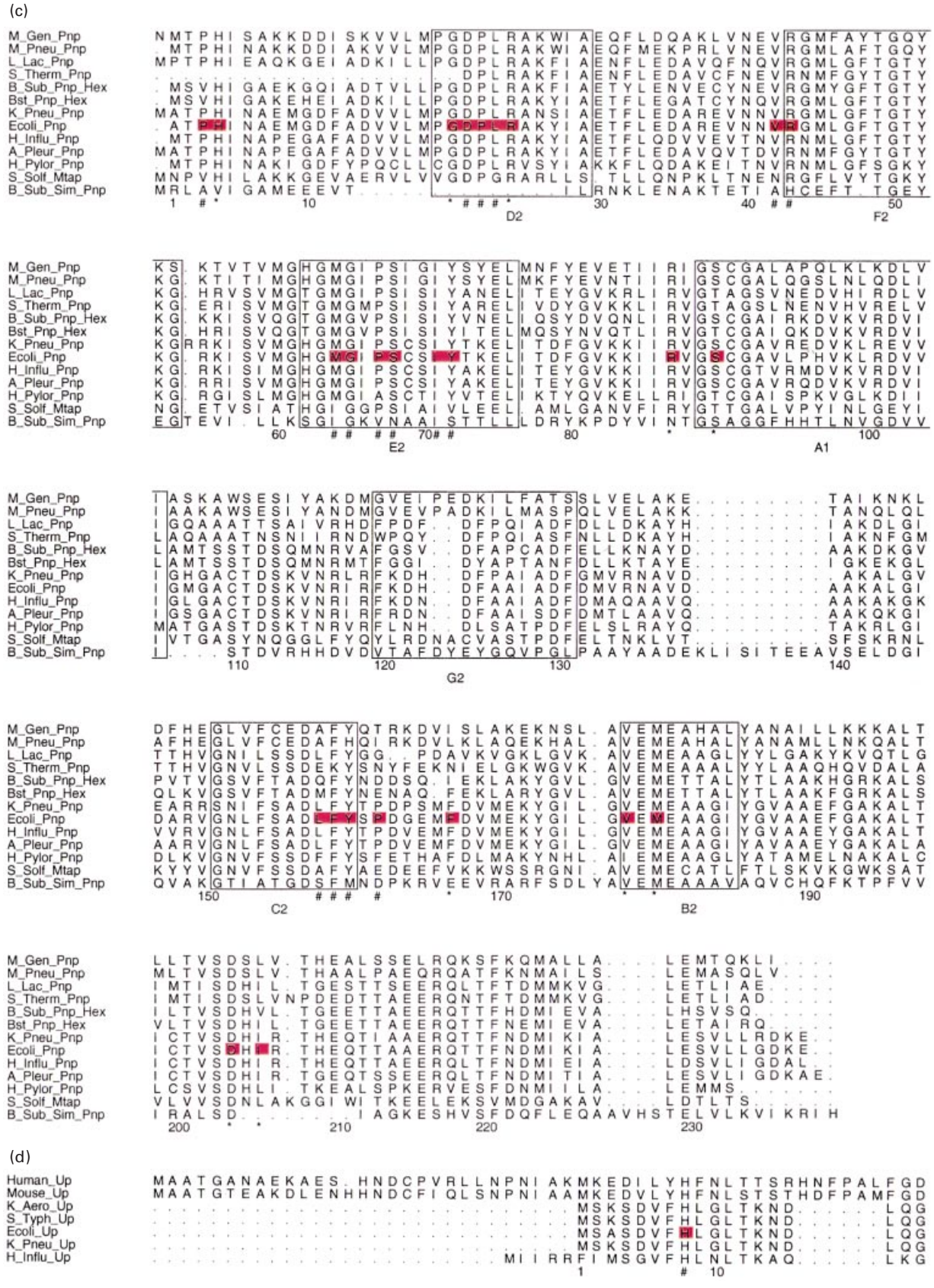

Figure 3 For legend see page 11

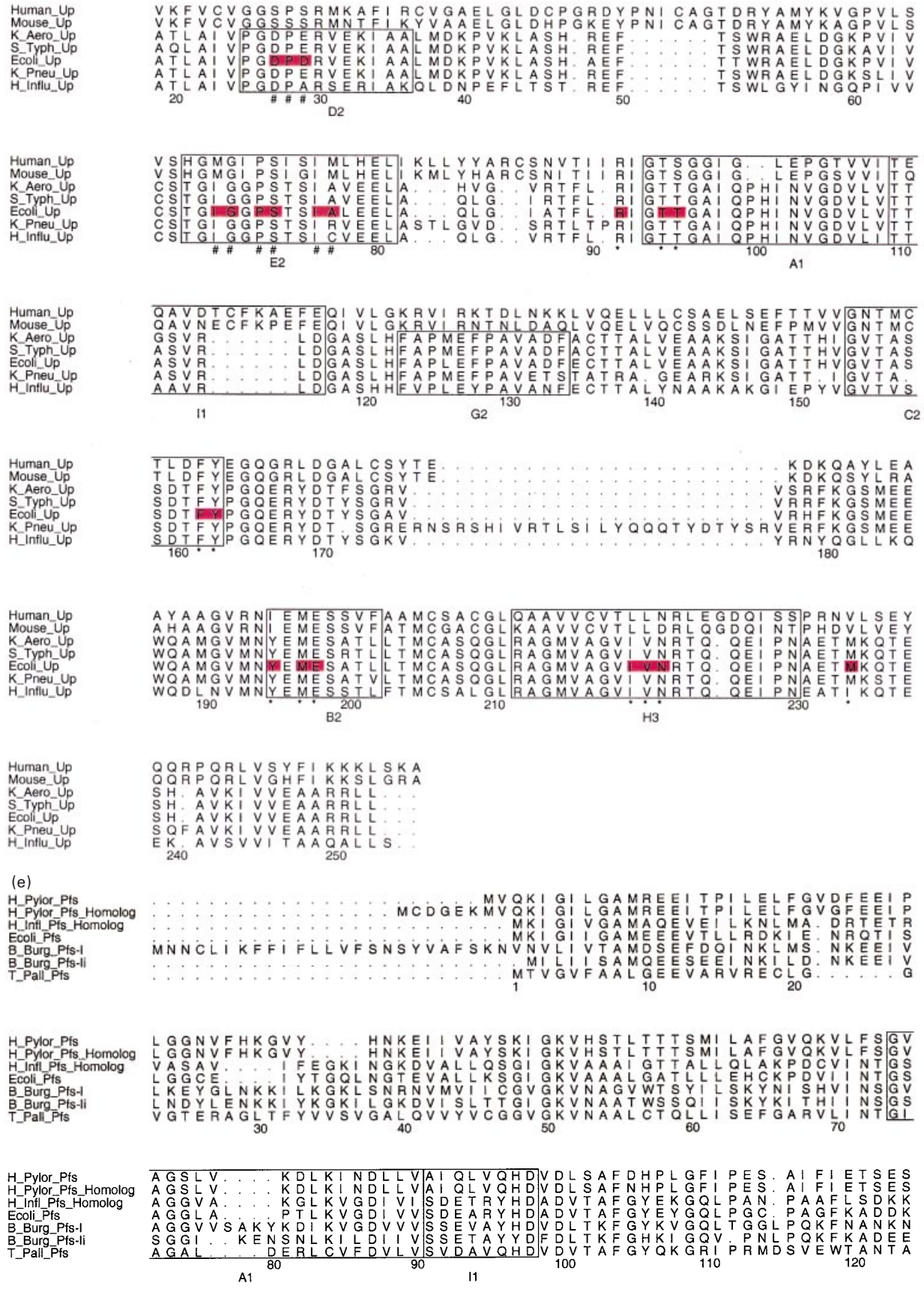

Figure 3 For legend see opposite

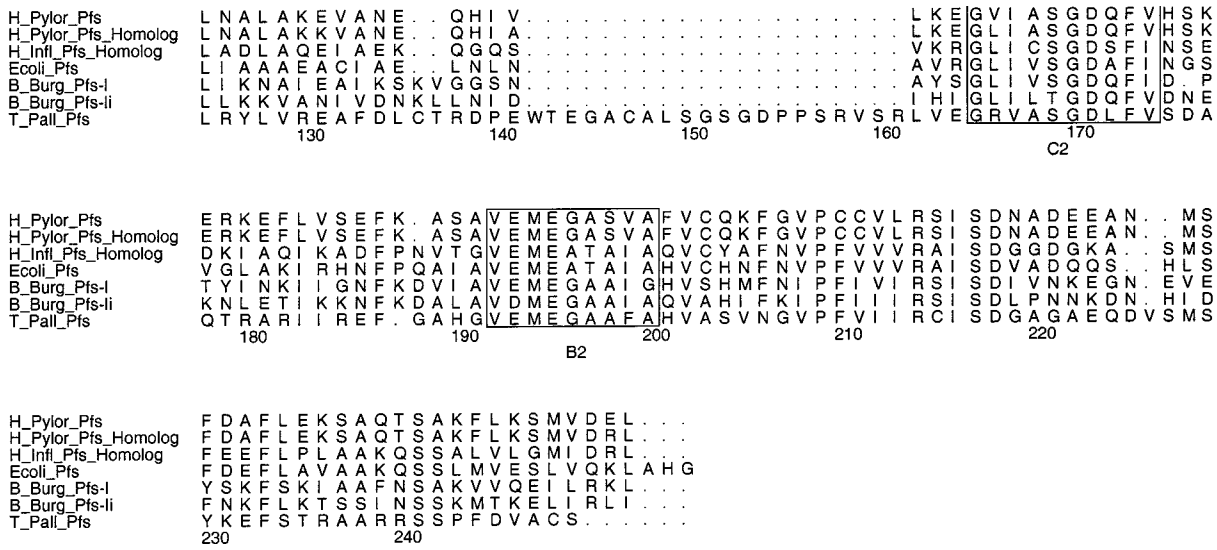

Figure 3 Multiple sequence alignments of each of the subfamilies in the NP-I family

Motif regions are boxed and labelled below the sequences. Residues of a representative sequence that are involved in the active site or in inter-subunit contacts are highlighted in red. Active-site residues are labelled as *, while those involved in subunit contacts are labelled as # (below the sequences). (**a**) Sequences from the trimeric PNP subfamily are labelled as: Bst_Pnp_Tri, trimeric PNP from *Bacillus stearothermophilus*; B_Sub_Pnp_Tri, trimeric PNP from *Bacillus subtilis*; Ecoli_Xp, *E. coli* xanthosine phosphorylase; H_Mouse_Pnp, house-mouse PNP; W_Mouse_Pnp, western wild mouse PNP; Bov_Pnp, bPNP; Hum_Pnp, hPNP; S_Cerv_Pnp, *Saccharomyces cerevisiae* PNP; M_Lep_Pnp, *Mycobacterium leprae* PNP. The numbering refers to the bPNP sequence. (**b**) Sequences from the MTAP subfamily are labelled as: M_Therm_Mtap, *Methanobacterium thermoautotrophicum* MTAP; M_Jann_Hypo, *Methanococcus jannaschii* hypothetical protein; A_Fulg_Mtap, *Archaeoglobus fulgidus* MTAP; C_Elegans_Mtap, *Caenorhabditis elegans* MTAP; Human_Mtap, hMTAP; S_Cerv_Orf, *Saccharomyces cerevisiae orf* gene; S_Cerv_Hypo, *Saccharomyces cerevisiae* hypothetical protein; S_Pombe_Hypo, *Schizosaccharomyces pombe* hypothetical protein; S_Sp_Hypo, *Synechocystis* sp. hypothetical protein; M_Tuber_Unk, *Mycobacterium tuberculosis* unknown; R_Rub_Hypo, *Rhodospirillum rubrum* hypothetical protein. The numbering refers to the hMTAP sequence. (**c**) Sequences from the hexameric PNP subfamily are labelled as: M_Gen_Pnp, *Mycoplasma genitalium* PNP; M_Pneu_Pnp, *Mycoplasma pneumoniae* PNP; L_Lac_Pnp, *Lactococcus lactic cremoris* PNP; S_Therm_Pnp, *Streptococcus thermophilus* PNP; B_Sub_Pnp_Hex, hexameric PNP from *Bacillus subtilis*; Bst_Pnp_Hex, hexameric PNP from *Bacillus stearothermophilus*; K_Pneu_Pnp, *Klebsiella pneumoniae* PNP; Ecoli_Pnp, *E. coli* PNP; H_Influ_Pnp, *Haemophilus influenzae* PNP; A_Pleur_Pnp, *Actinobacillus pleuropneumoniae* PNP; H_Pylor_Pnp, *Helicobacter pylori* PNP; S_Solf_Mtap, *Sulfolobus solfataricus* MTAP; B_Sub_Sim_Pnp, *Bacillus subtilis* protein similar to PNP. The numbering refers to the *E. coli* PNP sequence. (**d**) Sequences from the UP subfamily are labelled as: Human_Up, human UP; Mouse_Up, house-mouse UP; K_Aero_Up, *Klebsiella aerogenes* UP; S_Typh_Up, *Salmonella typhimurium* UP; Ecoli_Up, *E. coli* UP; K_Pneu_Up, *Klebsiella pneumoniae* UP; H_Influ_Up, *Haemophilus influenzae* UP. The numbering refers to the *E. coli* UP sequence. (**e**) Sequences from the uncharacterized subfamily are labelled as: H_pylor_Pfs, *Helicobacter pylori* pfs protein; H_pylor_Pfs_Homolog, *Helicobacter pylori* pfs homologue; H_infl_Pfs_Homolog, *Haemophilus influenzae* pfs homologue; Ecoli_Pfs, *E. coli* pfs protein; B_Burg_Pfs-I, *Borrelia burgdorferi* pfs_I; B_Burg_Pfs-Ii, *Borrelia burgdorferi* pfs_II; T_Pall_Pfs, *Treponema pallidum* pfs. The numbering refers to the *Treponema pallidum* pfs sequence. This Figure was created using ALSCRIPT [164].

purine nucleosides, whereas the hexameric PNPs accept adenosine in addition to 6-oxo purine nucleosides. MTAP is specific for 5′-methylthioadenosine, but will accept various substrate analogues such as 5′-methylselenoadenosine, 5′-ethylthioadenosine and 5′-n-propylthioadenosine [56,89]. UP accepts only pyrimidine nucleosides and lacks specificity at the 2′-ribose position in higher organisms [50]. However, UP will not cleave cytidine, which is not cleaved by any known nucleoside phosphorylase. Previous work in our laboratory has reported a detailed comparison of the active sites and substrate-binding modes in trimeric and hexameric PNPs [80], and showed that the trimeric and hexameric subfamilies have significant differences in the positions of active-site residues. Schematic diagrams representing the active sites in each of the subfamilies of NP-I are shown in Figure 5 (below). While the members of the NP-I family all bind P_i and a nucleoside, which subsequently undergo a phosphorolysis reaction, the modes of substrate binding show significant variation, and help to explain the differences in substrate specificity.

Binding of the phosphate ion is known to induce conformational changes in the loop regions between strand 1A and helix H2, and between strands 2A and 3A, of the bPNP structure [76]. When structures of trimeric and hexameric forms of PNP are superimposed, both the phosphate- and nucleoside-binding sites also superimpose, although the orientation of the phosphate with respect to the nucleoside in the hexameric PNPs is slightly different than in the trimeric forms. The phosphate-binding pocket is located at the C-terminal edge of the central β-sheet (see Figure 1c). The positioning of the active-site residues of each member of the NP-I family, after superimposing the phosphate ions of each structure, is shown in Figure 6. There is a significant similarity among the active-site residues of trimeric structures (hMTAP and bPNP), while the hexameric structures (*E. coli* PNP and UP, whose active site has not been as well characterized) appear to utilize different residues for binding the phosphate ion. In bPNP and hMTAP, several residues are structurally conserved and show the same phosphate-binding interactions. These include Ser-33 in bPNP and Thr-18 in hMTAP; Ala-116 and Ala-94; Ser-220 and Thr-197; and Arg-84 and Arg-60. The side chains of His-64 in bPNP and His-61 in hMTAP are also in the same position in binding the phosphate ion, but interestingly come from regions that are not structurally conserved. There is also an interaction in hMTAP between the side chain of Thr-93 and O-3 of the phosphate ion which corresponds to an interaction with a water molecule in bPNP. None of the other structures contain a residue that corresponds to His-86 of bPNP, which, along with Glu-89 and phosphate, form a possible catalytic triad. Of the active-site residues in the hexameric structures, only Ser-90 and Arg-87 of *E. coli* PNP occur in a region that is structurally conserved among all members

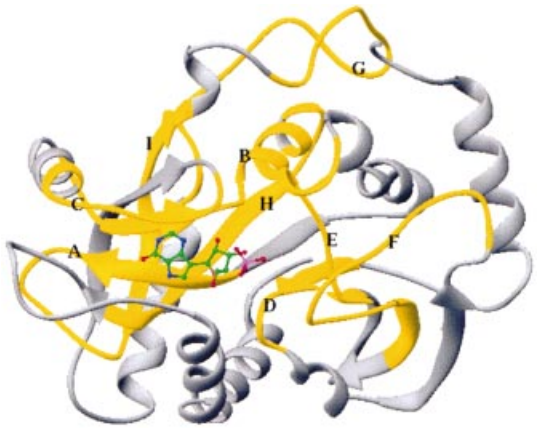

Trimeric	Hexameric	MTAP	UP
B_1.....a	B_2.....a,s	E_3.....a,s	H_3.....a
C_1.....a,s	C_2.....a,s	H_2.....a	I_1.....a
D_1.....a	D_2.....a		
E_1.....a,s	E_2.....a,s		
F_1.....a	F_2.....s		
G_1.....s	G_2		
H_1.....a			

Figure 4 Ribbon drawing of a subunit of bPNP showing the corresponding structural locations of the nine motif regions (coloured yellow and labelled A–I) found in NP-I sequences

The specific sequence motifs (indicated by their subscript number) that are specific for trimeric PNP, hexameric PNP, MTAP and UP sequences are each listed in their appropriate group. Each sequence motif is labelled as being involved in the active site (a) and/or being involved in subunit interactions of the quaternary structure (s). The Figure was created with RIBBONS [163].

of the NP-I family. It is significant that these two residues occur in the highly conserved β-strand and loop region (motif A_1 corresponding to strands 1B and 6A, and the interconnecting loop). The rest of the phosphate-binding residues in the hexameric structures (including two arginine residues) come from loop regions that are not structurally conserved, or from a helix that is only conserved among hexameric structures.

The nucleoside-binding pocket is also located along the C-terminal edge of the central β-sheet, adjacent to the phosphate-binding site (see Figure 1c). A large flexible loop region (residues 246–265) in bPNP and hPNP may act as a gate that allows the entrance and exit of substrates and reaction products [32]. Part of this loop region undergoes a significant structural change when nucleoside binds, where the N-terminus of helix H7 is extended to include residues 257–265. The corresponding loop in the hexameric structures is much shorter and does not undergo a similar transition. The positioning of the active-site residues of each member of the NP-I family, after superimposing their nucleoside substrates, is shown in Figure 6. The residues that interact with the ribose moiety show a significant similarity in the group of methionine residues from all four structures that form a hydrophobic interaction with the ribose ring. The corresponding methionine in bPNP (Met-219) occurs in a loop following β-strand 4B. Although this region is not structurally conserved among trimeric and hexameric structures, the corresponding residues are close enough to effectively position the methionine side chains in the same general location near the ribose ring. This methionine is absolutely conserved in all known sequences of the NP-I family. Another significant similarity involves active-site residues that participate in a hydrophobic pocket near the 5′ position of the ribose ring. His-137 from

Table 2 Highly conserved sequence motifs found in the NP-I sequences

The structural location of each motif is indicated by its label with reference to Figure 4. For each motif, the residue numbers from one representative sequence with known three-dimensional structure are listed for reference. The corresponding structural and functional significance is also listed for each motif.

Motif	Residues	Structural/functional significance
A		
A_1	115–131 (bPNP)	Involved in active site
B		
B_1	213–229 (bPNP)	Involved in active site
B_2	178–185 (*E. coli* PNP)	Involved in active site and in hexameric contacts
C		
C_1	197–205 (bPNP)	Involved in active site and in trimeric contacts
C_2	151–160 (*E. coli* PNP)	Involved in active site and in hexameric contacts
D		
D_1	27–35 (bPNP)	Involved in active site
D_2	19–29 (*E. coli* PNP)	Involved in active site and in hexameric contacts
E		
E_1	81–91 (bPNP)	Involved in active site and in trimeric contacts
E_2	62–76 (*E. coli* PNP)	Involved in active site and in hexameric contacts
E_3	60–82 (hMTAP)	Involved in active site and in trimeric contacts
F		
F_1	53–71 (bPNP)	Involved in active site
F_2	43–54 (*E. coli* PNP)	Involved in hexameric contacts
G		
G_1	145–167 (bPNP)	Involved in trimeric contacts
G_2	120–131 (*E. coli* PNP)	None
H		
H_1	230–243 (bPNP)	Involved in active site
H_2	207–224 (hMTAP)	Involved in active site
H_3	212–230 (*E. coli* UP)	None
I		
I_1	102–117 (*E. coli* UP)	Involved in active site

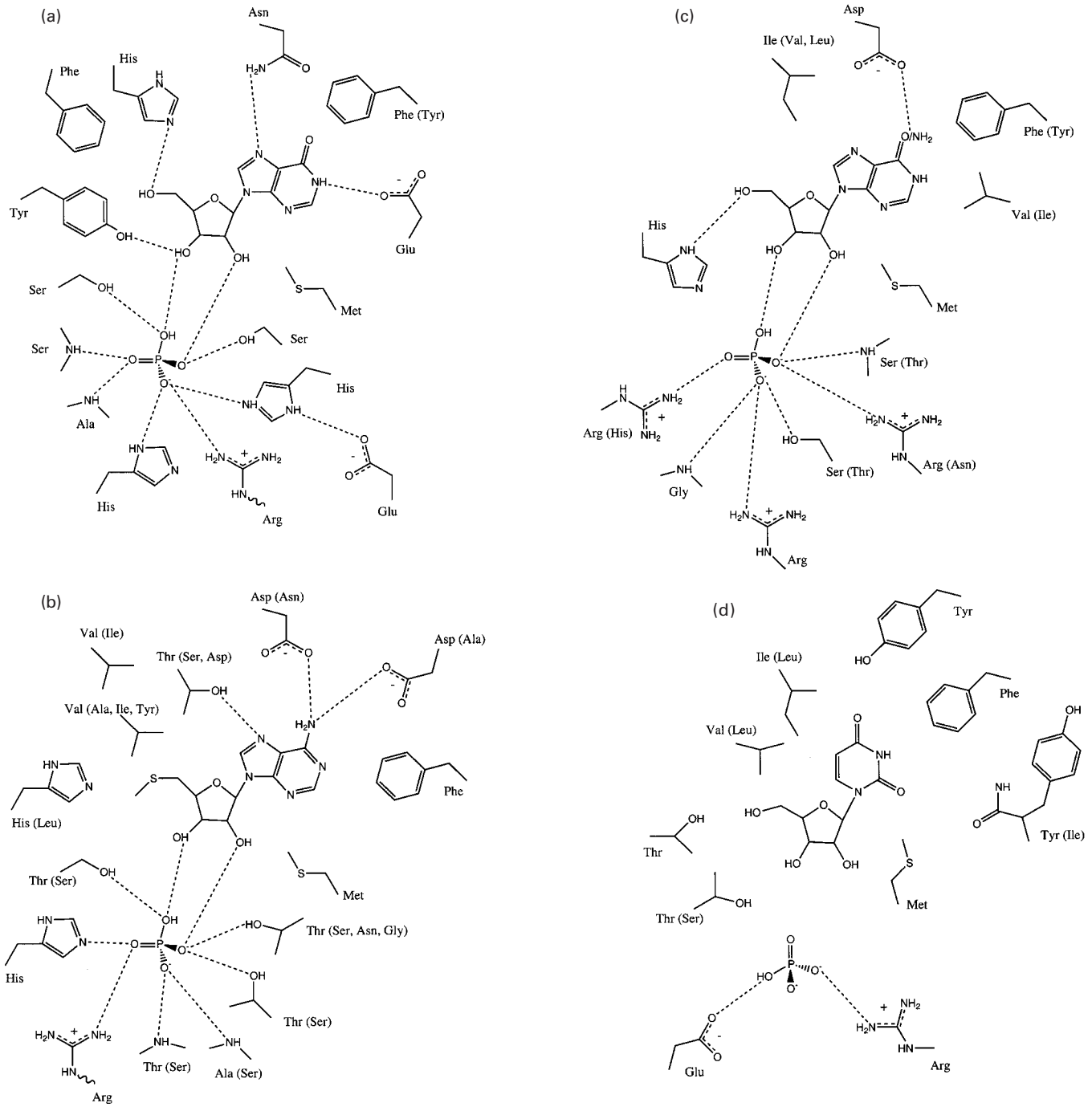

Figure 5 Schematic drawings of a representative active site of each NP-I subfamily

(**a**) Trimeric PNP, (**b**) MTAP, (**c**) hexameric PNP, and (**d**) UP, whose active site has not been well characterized. Shown are the residues that are thought to be involved in substrate binding. Residues that are absolutely conserved in the subfamily are indicated, while those residues that are variable show the most common variants in parentheses.

hMTAP, Phe-159 from bPNP and His-4 from *E. coli* PNP all come from neighbouring subunits of the PNP molecule. His-137 and His-159 are structurally conserved in hMTAP and bPNP (in a large loop between β-strand 2B and helix H4 in bPNP), while His-4 in *E. coli* PNP comes from a completely different region of the PNP fold. His-257, which is part of the large flexible loop in bPNP, is also near this position, where it binds the 5′-OH of the ribose ring and subsequently participates in the conformational change in residues 257–265 discussed above. It is significant that no other residues in the other structures correspond to His-257. Val-233 of hMTAP is in roughly the same position, but is involved in a hydrophobic pocket that probably contributes to the binding of the 5′-deoxy-5′-methylthio group of MTAP substrates.

Significant similarities in residues that are involved in base binding include the herringbone stacking interaction that involves

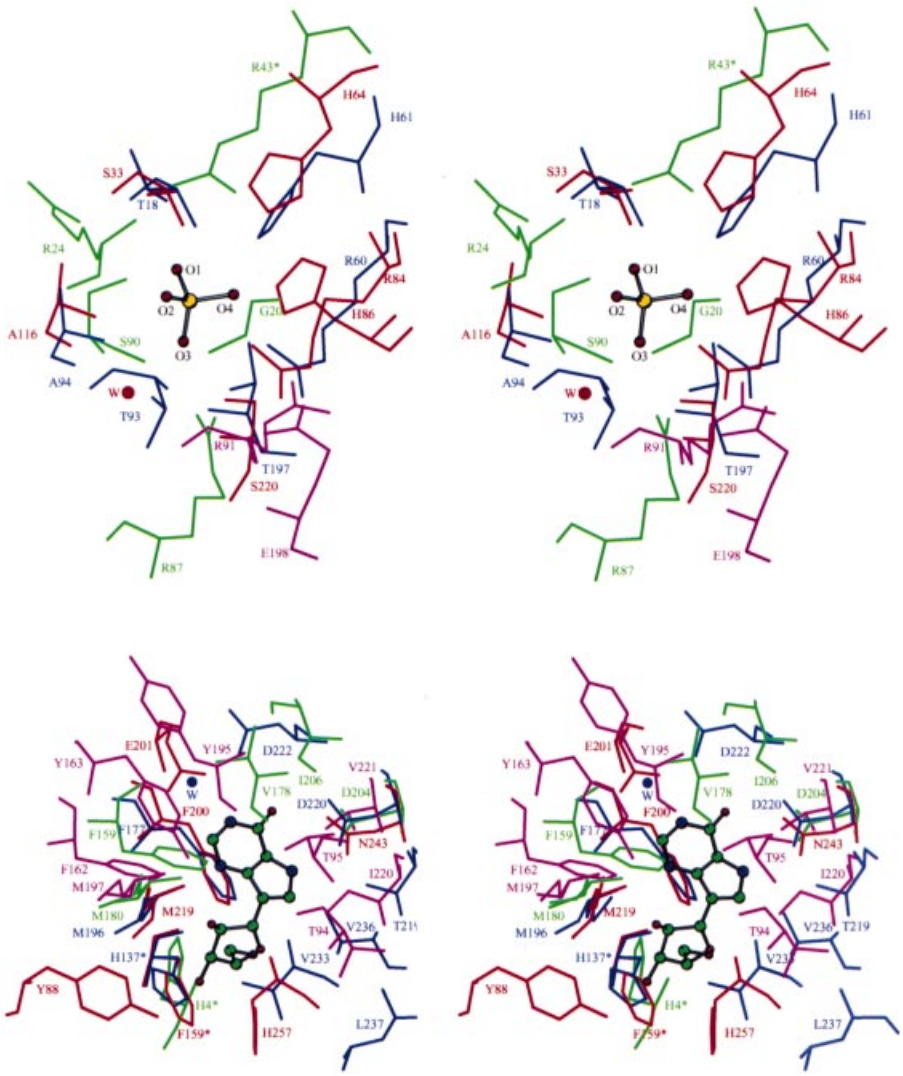

Figure 6 Superposition of the active-site residues from structures of the NP-I family

The residues are labelled and coloured as follows: red, bPNP; blue, hMTAP; green, *E. coli* PNP; violet, *E. coli* UP. Upper panel, phosphate-binding site; lower panel, nucleoside-binding site. The Figure was produced with MOLSCRIPT [162].

Phe-200 of bPNP, Phe-177 of hMTAP, Phe-159 of *E. coli* PNP and Phe-162 of *E. coli* UP. Of these residues, only those from bPNP and hMTAP are structurally conserved (in a loop between β-strand 3B and helix H5 in bPNP), although the side chains in both trimeric and hexameric structures are positioned to be perpendicular to the plane of the purine or pyrimidine base. The interaction between Glu-201 of bPNP and N-1 of the purine base corresponds to an interaction with a water molecule in hMTAP; no residues from the hexameric structures form interactions at this position. The majority of the base specificity is likely to occur at the 6-position, where residues of all four structures are in structurally conserved positions in β-strand 5B. The aspartic acid side chains in hMTAP and *E. coli* PNP (Asp-220 and Asp-204 respectively) allow for hydrogen bonding with the 6-amino purine nucleosides, while Asn-243 of bPNP specifies 6-oxo purine nucleosides. Val-221 in this position in *E. coli* UP is probably contributing to a hydrophobic pocket thought to be near the 5-position of the pyrimidine ring. Asp-222 of hMTAP is also in a position to hydrogen-bond with the 6-amino position of the MTAP substrates.

A study based on structural and kinetic analyses of a trimeric PNP has suggested a possible catalytic mechanism for hPNP [64] that is likely to be similar in all members of the NP-I family. Several bPNP–substrate-analogue complexes have been solved in our laboratory, and these suggest that the β-nucleoside binds in a high-energy $+$*anticlinal* torsion angle of the glycosidic bond, with the ribose moiety in the uncommon C-4′-*endo* sugar pucker [76]. The proposed mechanism for hPNP suggests that this high-energy conformation produces steric strain, which encourages glycosidic cleavage. The glycosidic bond is weakened further as electrons flow from O-4′ of the ribose to the purine ring, and this results in an oxocarbenium ion that is stabilized by the negative charges of the phosphate ion. The phosphate ion binds on the α-side of the ribose ring, where it is positioned to participate in an S_N1 nucleophilic attack at the C-1′ position. The flow of electrons from the glycosidic bond to the purine ring is probably stabilized

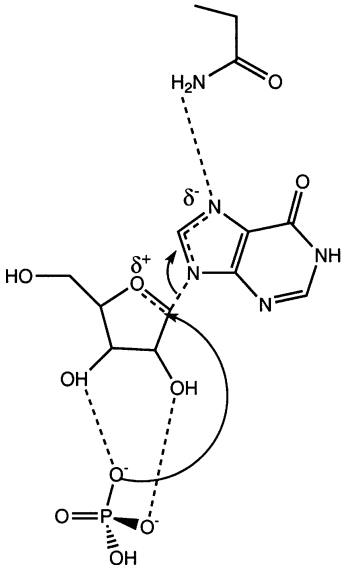

Figure 7 Proposed catalytic mechanism for hPNP, representative of a likely mechanism for all NP-I family enzymes

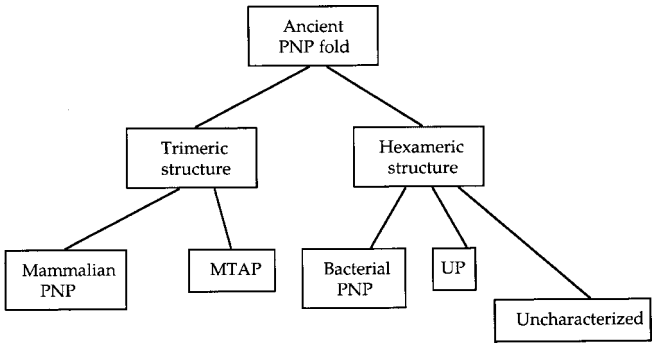

Figure 8 Possible evolutionary pathway of the NP-I family, based on sequence and structural analyses

by active-site-residue interactions at the N-7 position. A recent structural study by Fedorov et al. [66] provided additional details of the atomic motions that are responsible for catalysis. The analogous flow of electrons to the pyrimidine ring in *E. coli* UP is likely to be stabilized by hydrogen-bond-donor interactions with the O-2 and O-4 positions. A schematic diagram of the proposed catalytic mechanism in hPNP is shown in Figure 7, and is representative of a likely mechanism for all members of the NP-I family.

NP-I EVOLUTIONARY ASPECTS

Protein structure is often conserved among distant members of a protein family, although the nucleotide sequences have diverged beyond recognition. Structural information, when available, can thus serve as a much more sensitive probe in determining ancient relationships than sequence identity alone. The NP-I family shows a conserved subunit fold, even though there is a quaternary structural division between trimeric and hexameric forms. Although the sequence identity between members of the trimeric and hexameric subfamilies is below the level normally used to establish an evolutionary relationship, the structural similarity confirms their relationship. Based on the division between the trimeric and hexameric subfamilies with regard to their overall sequence, as well as in sequence motifs, a phylogenetic scheme is suggested as shown in Figure 8. A likely early evolutionary event was the divergence of an ancient NP-I fold into trimeric and hexameric family members. The trimeric structure continued to diverge and specialize, resulting in the PNPs that are now commonly found in eukaryotes as well as some prokaryotes, and the MTAP structure that is found in a variety of organisms. The hexameric family may also have diverged, resulting in the hexameric PNP structure found only in prokaryotic cells and the hexameric UP structure that is found in a variety of organisms. In addition, the hexameric subfamily of NP-I may also have diverged into a third category of as yet uncharacterized hypothetical proteins. The evolutionary pathway in Figure 8 suggests divergent evolution from a common ancestor that perhaps accepted a wide range of nucleoside and/or nucleotide substrates and then became more specialized for particular nucleosides over time. It is also possible, however, that the NP-I family resulted from convergent evolution, whereby the enzymes that we know today have evolved from several disparate sources. In this case, the common folds of the NP-I family would have been formed independently, as a result of the need to catalyse similar reactions with similar substrates.

Iterative BLAST searches starting with various members of the NP-I family reveal similarities between the monomer fold and both MTA/SAH nucleosidase and AMP nucleosidase. The similarity is greatest between the nucleosidases and the hexameric NP-I family members. Like nucleoside phosphorylases, nucleosidases cleave the glycosidic bond; however, unlike nucleoside phosphorylases, nucleosidases utilize water as the nucleophile. Further examination of the nucleosidase sequences revealed that several key residues in the nucleoside-binding site were conserved. However, all three arginine residues, which account for most of the phosphate-binding site in the nucleoside phosphorylases, have been replaced by neutral amino acids. The similarity to the NP-I family has now been confirmed by the crystal structure of MTA/SAH nucleosidase from *E. coli* [90]. The structure shows that the fold is indeed conserved but, in contrast with the other NP-I members, MTA/SAH nucleosidase is dimeric. The structure of AMP nucleosidase has not yet been determined.

PNP INHIBITOR DESIGN

Inhibitors of PNP have the potential to help prevent the degradation and deactivation of nucleoside analogues used in chemotherapeutic treatments [91,92]. PNP deficiency has additionally been linked to several immunological diseases, such as T-cell immune deficiency [31,93,94]. Inhibitors of PNP have the potential to suppress the T-cell response in T-cell proliferative diseases such as T-cell lymphoma and T-cell leukaemia, as well as in T-cell-related autoimmune diseases such as rheumatoid arthritis and lupus. This method of suppressing T-cells may also find application in organ transplantation, where the donated organ is often rejected due to a massive T-cell response. Despite the potential benefits of a potent inhibitor of PNP activity, thus far no drug has reached the clinic.

Effective *in vivo* inhibitors have been difficult to obtain, presumably due to the high levels of PNP in humans, particularly in lymphoid tissues and in erythrocytes, which necessitates a very potent binding affinity. One of the first known inhibitors of PNP was the guanine analogue 8-aminoguanine, which showed a K_i of

0.2 μM [30] with human erythrocyte PNP. Prompted by its structural similarity to the natural substrates of PNP, the antiherpetic agent acyclovir and its metabolites, which belong to the class of nucleoside analogues known as acyclic nucleosides, were also tested for PNP inhibition and shown to have significant binding properties. Tuttle and Krenitsky [95] showed that the phosphorylated metabolites of acyclovir, using a physiological phosphate concentration of 1 mM, had K_i values of 6.6, 0.0087 and 0.31 μM for the mono-, di- and tri-phosphate esters respectively. A later study [96] of acyclovir phosphate metabolites further investigated their binding properties with PNP, and showed that the inter-atomic distance between the carbon of the 9-substituent of the guanine and the terminal oxygen anion is a critical factor in determining binding affinity for hPNP. That study showed the diphosphate to be of optimal length, explaining why it binds better than the mono- or tri-phosphate acyclovir esters. Despite the favourable binding properties of acyclovir diphosphate, its inability to permeate membranes and its susceptibility to metabolism limit its potential as a clinically useful drug. Other nucleoside analogues that have been tested for inhibition of PNP include a series of 9-phosphonoalkylhypoxanthines, of which the most effective showed a K_i of only 0.9 μM [97]. In addition, many ring analogues of guanine and hypoxanthine and the corresponding nucleosides have been tested for PNP inhibition, but, with the exception of the 9-deazapurines, none are as effective as the 8-aminoguanine compounds discussed above [98].

The first attempts to rationally design PNP inhibitors based on the three-dimensional structure of the enzyme were reported by Ealick and co-workers [32]. The crystal structures of PNP in complex with several known potent nucleoside analogue inhibitors revealed important hydrogen-bonding patterns in the base-binding site involving residues Glu-201, Thr-242 and Asn-243, and showed the interactions in the ribose-binding site to be largely hydrophobic. Structures of complexes also showed how the 8-amino group enhanced binding in guanine analogues, but had the opposite effect in 9-deazaguanines. This study [32] also verified that the acyclovir diphosphate was indeed a multisubstrate inhibitor, occupying the base- and phosphate-binding sites. The crystal structure of hPNP in complex with acyclovir diphosphate showed the spacer length between N-9 and the phosphate ion to be optimal for occupying both the base- and phosphate-binding sites. These structural studies suggested that optimal inhibitors of PNP would take advantage of the base-, ribose- and phosphate-binding sites. This prompted further rational design efforts using iterative cycles of modelling of potential inhibitors into the active site of the hPNP structure, synthesis of potentially high-affinity compounds, and testing of the compounds using X-ray structure determination and measurement of specific binding affinities. These efforts resulted in a series of 9-substituted 9-deazapurine analogues with various aromatic, heteroaromatic and cyclic aliphatic substituents that would occupy the hydrophobic ribose-binding site, followed by a substituent that would have affinity for the phosphate-binding site. The first set of studies focused on a series of 9-(arylmethyl) derivatives of 9-deazaguanine, which showed IC_{50} values that ranged from 17 to 120 nM; 9-(3,4-dichlorobenzyl)-9-deazaguanine was the most potent of this series [99]. Further studies demonstratedd a series of 9-alicyclic and 9-heteroalicyclic derivatives of 9-deazaguanine to have similar IC_{50} values; 9-(2-tetrahydrothienylmethyl)-9-deazaguanine showed the highest affinity for hPNP, with an IC_{50} of 11 nM [100]. Continued studies resulted in a series of 9-(arylmethyl)-9-deazaguanine analogues that were substituted at the methylene group. This resulted in the highest-affinity compound of this work: the membrane-permeant PNP inhibitor (*S*)-9-[1-(3-chlorophenyl)-2-carboxyethyl]-9-deazaguanine, which had an IC_{50} of 5.9 nM in an *in vitro* assay [101,101a]. The results of these studies suggested that the optimum spacer between the hydrophobic and the phosphate-binding regions is 2–4 carbon atoms, and that between the purine ring and the hydrophobic substituent is a single methylene group. It was also shown that acyclic hydrophobic substituents at the 9-position alone were poor inhibitors, which suggested that a rigid structure is necessary in the hydrophobic ribose-binding pocket.

The favourable characteristics of the binding of acyclovir diphosphate to hPNP, in addition to its lack of stability *in vivo*, have prompted additional X-ray structural studies based on analogues of acyclovir diphosphate [102]. The study tested various phosphate mimics, including sulphonic acid and carboxylic acid groups, which interact favourably with the phosphate-binding site in hPNP. This resulted in the synthesis of 9-(3,3-dimethyl-5-phosphonopentyl)guanine, which has an IC_{50} of 44 nM. Kelley and co-workers [103] synthesized and tested a series of {[(guaninylalkyl)phosphinoco]methyl}phosphonic acids in an effort to produce an acyclovir diphosphate analogue that was stable *in vivo* while retaining high affinity for hPNP. The most potent compound of this series was ({[5-(2-amino-1,6-dihydro-6-oxo-9H-purin-9-yl)pentyl]phosphinoco}methyl)-phosphonic acid, which showed a K_i of 3.1 nM and required Zn^{2+} ions for optimal activity, but showed only weak activity against human leukaemic T-cells *in vitro*. A recent study, which focused on designing transition-state analogues of PNP, has produced the most potent inhibitors thus far [104]. These inhibitors incorporate features of the transition state, including an elevated pK_a at N-7 of the purine ring and a positive charge in the ribose ring that mimics the formation of an oxocarbenium. The most potent compounds are (1*S*)-1-(9-dezahypoxanthin-9-yl)-1,4-dideoxy-1,4-imino-D-ribitol (immucillin-H) and (1*S*)-1-(9-deazaguanin-9-yl)-1,4-dideoxy-1,4-imino-D-ribitol (immucillin-G), which showed K_i values that ranged from 23 to 72 pM when tested against calf spleen and human erythrocytic PNP. Further studies are required to determine if such compounds will be successful in the clinic.

NP-II FAMILY

Following the discovery of a distinct enzyme for the phosphorolysis of pyrimidines, several studies characterized PyNP further. Several works confirmed the suggestion by Paege and Schlenck [12] that there existed two separate PyNPs. Laster and Blair [105], for example, reported that a UP from mammalian tissue did not distinguish between the ribose moieties of uridine and thymidine, while a distinct TP was specific for the 2′-deoxyribose moiety of thymidine. The work of Krenitsky and coworkers [50] solidified this hypothesis and established a general definition of the two major classes of PyNPs: TP and UP. This study, which included PyNPs from a broad range of bacterial and mammalian species, again confirmed the presence of two distinct pyrimidine-cleaving enzymes. Nevertheless, it was shown that the specificity for the ribose moiety, as well as the specificity at the 5-position of the pyrimidine ring, varied among species. TP was also reported to be distinct in its pH optima, as the TP class had a general pH optimum of 5.5.

The deoxyribosyltransferase activity was attributed to TP in the works of Zimmerman and Seidenberg [106,107]. Later studies verified this activity, and also showed that deoxyribose 1-phosphate and the pyrimidine base bind at two distinct locations in the enzyme [108]. It was further shown [109] that the deoxyribose 1-phosphate is a free intermediate, so that the

transferase activity, involving two pyrimidine bases B1 and B2, is likely to take place via a two-step mechanism as follows (where dR is deoxyribose and dR-1-P is deoxyribose 1-phosphate):

$$\text{B1-dR} + \text{P}_\text{i} \leftrightarrow \text{B1} + \text{dR-1-P}$$

$$\text{dR-1-P} + \text{B2} \leftrightarrow \text{B2-dR} + \text{P}_\text{i}$$

TP and UP have now been isolated and characterized from a wide variety of species. In all cases, TP functions as a dimer, ranging in molecular mass from 80 kDa in *Lactobacillus casei* [110] to 110 kDa in human blood platelets [111], while UP functions as a hexamer, with a reported molecular mass of 165 kDa in *E. coli* [112]. Structural analysis indicates that *E. coli* UP belongs to the NP-I family, as discussed above. These studies suggest that the discriminating feature between UP and TP is the high specificity of TP for the 2′-deoxyribose moiety. TPs from rat liver [113], mouse liver [51], horse liver [10], *E. coli* [114], and *Lactobacillus casei* [110] have shown such specificity for the 2′-deoxyribose moiety. In all cases, the 5-position of the pyrimidine ring was less important in determining specificity than was the 2′-position of the ribose moiety. Several organisms, such as *Bacillus stearothermophilus* [115] and *Haemophilus influenzae* [116], however, are reported to contain a single PyNP that does not discriminate at the 2′-position of the ribose. Enzymes that accept both thymidine and uridine as substrates are referred to as PyNPs. PyNPs and TPs show significant sequence similarity and have similar physical properties. Our X-ray crystallographic studies showed that the three-dimensional structures of *Bacillus stearothermophilus* PyNP [117] and *E. coli* TP [118,119] are also similar.

Kinetic studies of TP from several species generally agree on a sequential mechanism. Studies of TP from *E. coli* [109] and rabbit muscle [120] suggest an ordered sequential mechanism, with phosphate binding before thymidine, and thymine being released before deoxyribose 1-phosphate. These results are corroborated by evidence that phosphate or deoxyribose 1-phosphate stabilizes the enzyme, but thymidine or thymine does not [121]. TP from *Lactobacillus casei* [110] shows a sequential mechanism with a random order of addition but an ordered release of products, where the release order is the same as that seen in *E. coli* and rabbit muscle enzymes. Mouse liver TP is reported to have a sequential mechanism with random order for both addition and release [122].

The expression of TP, like that of PNP and other nucleoside-binding enzymes, is inducible by the addition of deoxyribonucleosides. This induction suggests that these enzymes may share common regulatory factors. Further evidence suggests that this induction effect is due to the formation of deoxyribose 5-phosphate [123]. More recently, TP activity has also been reported to be inducible by interferon and other cytokines in several cancer cell lines [124,125]. Recently, increased interest in TP has focused on several intriguing findings. Platelet-derived endothelial cell growth factor, characterized by its angiogenic and endothelial cell chemotactic activities, was shown to be identical with human TP [126]. Similarly, gliostatin, characterized by its inhibition of glial cell growth and subsequent stimulation of neuronal survival, was also shown to be identical to human TP [127]. The relationship between these growth-factor activities and the phosphorylase activity is as yet unknown. TP is expressed in a wide variety of human tissues, with levels of expression varying up to 15-fold in different tissues. It is significant that TP levels in carcinomas of the stomach, breast, colon and ovary are elevated up to 10-fold in comparison with those in the corresponding non-neoplastic tissue [128–132]. This increase in activity in malignant tissue is likely to be associated with the growth-factor activity of TP. In view of these recent findings, understanding the structure–function relationship of TP has become an even more important focus.

NP-II STRUCTURES

Detailed structural information on the NP-II family was initially provided by the 2.8 Å crystal structure of *E. coli* TP [119]. The three-dimensional structure of TP reveals an S-shaped homodimer in which each subunit contains a large mixed α-helical and β-sheet domain (the α/β-domain) which is separated from a smaller α-helical domain (the α-domain) by a large cleft (Figure 9). Three loop regions connect these two domains. This fold represents a unique α/β-fold that is unrelated to the fold observed in the NP-I family. The topology of the NP-II fold is shown in Figure 10. The active site of each subunit consists of a thymidine-binding site in the α-domain and a phosphate-binding site across the cleft in the α/β-domain. The large distance between the phosphate- and thymidine-binding sites (8 Å) reported in *E. coli*

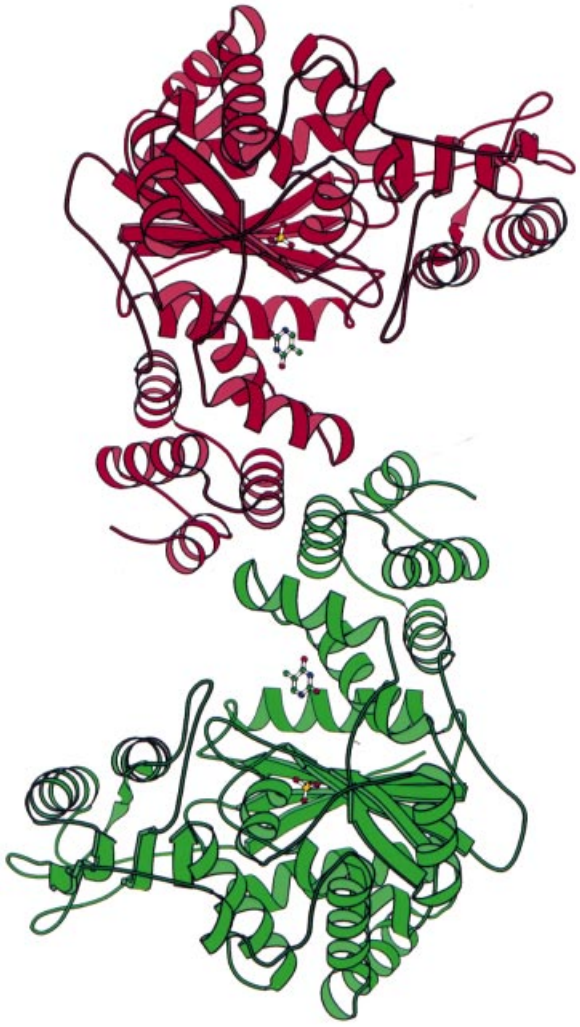

Figure 9 Ribbon drawing of the dimeric structure of *E. coli* TP in an open conformation

Crystallographically observed thymine and phosphate are shown as ball-and-stick models to indicate the positions of the binding sites in each of the subunits. The Figure was produced with MOLSCRIPT [162].

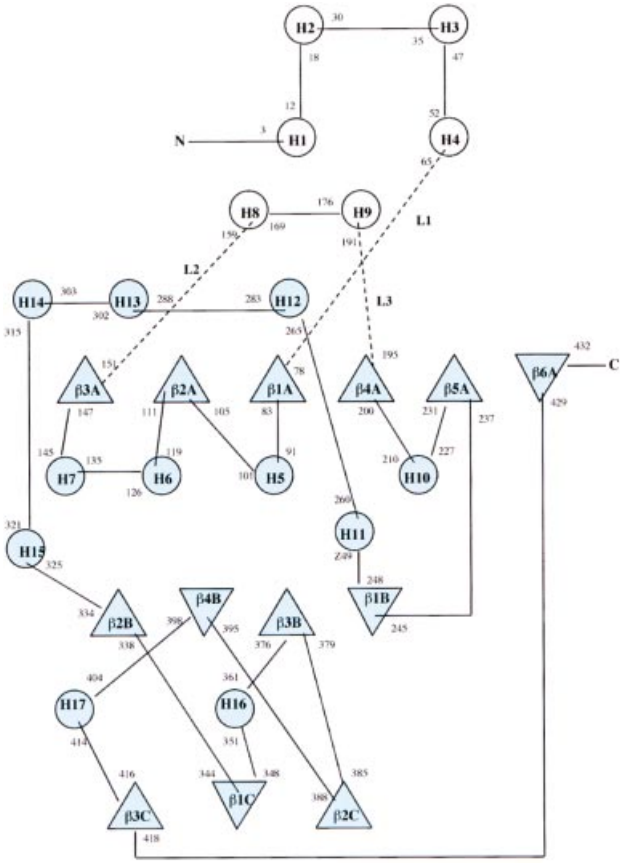

Figure 10 Topology diagram of the structure of PyNP from *B. stearothermophilus*, which is representative of the NP-II fold

Helices are represented as circles and β-strands as triangles. Secondary-structural elements of the α-domain are white and those of the α/β-domain are blue. The broken lines indicate the loop regions that connect the α- and α/β-domains. The first and last residue numbers of each secondary-structural element are indicated.

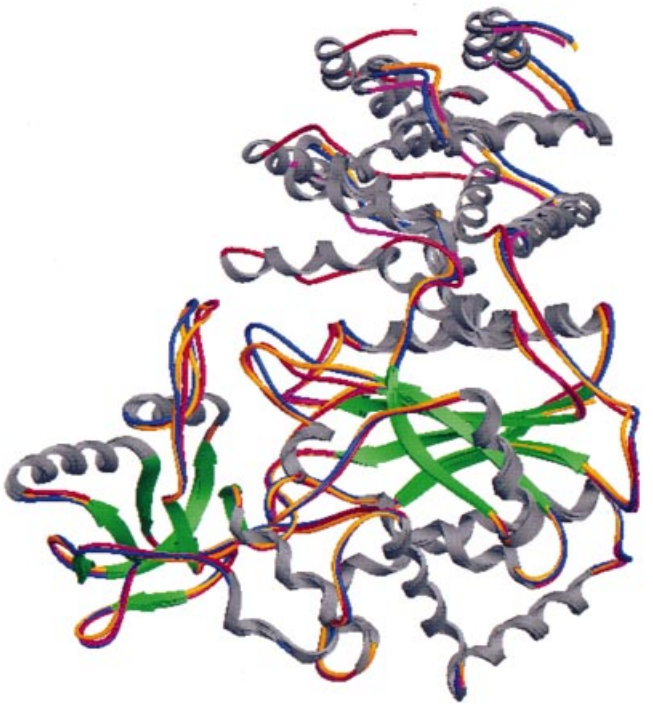

Figure 11 Ribbon drawing of the superposition of a single subunit from the known structures of the NP-II family where the α/β-domains have been aligned

The β-strands of all models are coloured green, and the α-helices are coloured grey. The colouring of the loop regions distinguishes each model as follows: red, *B. stearothermophilus* PyNP in the closed-cleft conformation; blue, monoclinic form of *E. coli* TP; yellow, orthorhombic form of *E. coli* TP; violet, tetragonal form of *E. coli* TP.

TP suggested that rigid-body domain movement, where the loop regions connecting the two domains act as hinge regions, may be necessary to close the cleft and enable catalysis to proceed. The structure solution of *E. coli* TP in three different crystal forms provided evidence for a domain movement [118] in which the domains move as rigid bodies. The monoclinic crystal form of *E. coli* TP showed the enzyme in the most open conformation, the orthorhombic form was intermediate, and the tetragonal form, which showed a sulphate ion bound in the phosphate-binding site, was the most closed. Further evidence for domain movement and subsequent cleft closure was obtained when we solved the crystal structure of PyNP from *B. stearothermophilus* in complex with phosphate and the substrate analogue inhibitor pseudouridine in a completely closed conformation [117]. These structures suggest that binding of phosphate causes an initial 8° rotation of the α/β-domain. Binding of the pyrimidine causes an additional 20° rotation, which produces a closed-cleft active conformation of the enzyme. The different relative orientations of the α- and α/β-domains observed in the TP and PyNP structures are shown in Figure 11. The crystal structure of PyNP in the closed conformation suggests a functional role for the dimeric structure, whereby side-chain residues from the α/β-domain form interactions across the cleft with residues from the α-domain of the other subunit.

NP-II ACTIVE SITE

The phosphate-binding pocket is located between two β-strands near the C-terminal end of the central β-sheet of the α/β-domain. Residues that bind phosphate come from these two strands as well as from a nearby loop. Phosphate binding causes the loop region comprising residues 115–120 in *E. coli* TP to become ordered, resulting from the formation of a key hydrogen bond between His-119 and Gly-208. This step is thought to be responsible for the initial 8° rotation of the α/β-domain. The pyrimidine-binding pocket is formed from residues in the two helices on the face of the α-domain facing the cleft. The primary interactions include binding of the two carbonyl groups of the pyrimidine ring by positively charged arginine and lysine residues, as well as a herringbone base-stacking interaction between the pyrimidine base and a tyrosine residue. Binding of the pyrimidine base in the α-domain is thought to interrupt a salt bridge between Lys-187 and Asp-161 in *B. stearothermophilus* PyNP. This allows the formation of a β-turn in one of the inter-domain connecting loops and is responsible for rotating the α/β-domain an additional 20° into its fully closed position.

The crystal structure of PyNP from *B. stearothermophilus* has identified active-site residues thought to be involved in binding the substrates, as shown in Figure 12. The active-site residues shown in Figure 12 are highly conserved among all sequences of the NP-II family (discussed below). The PyNP crystal structure provides an example of a member of the NP-II family that accepts both thymidine and uridine. Comparison of the active

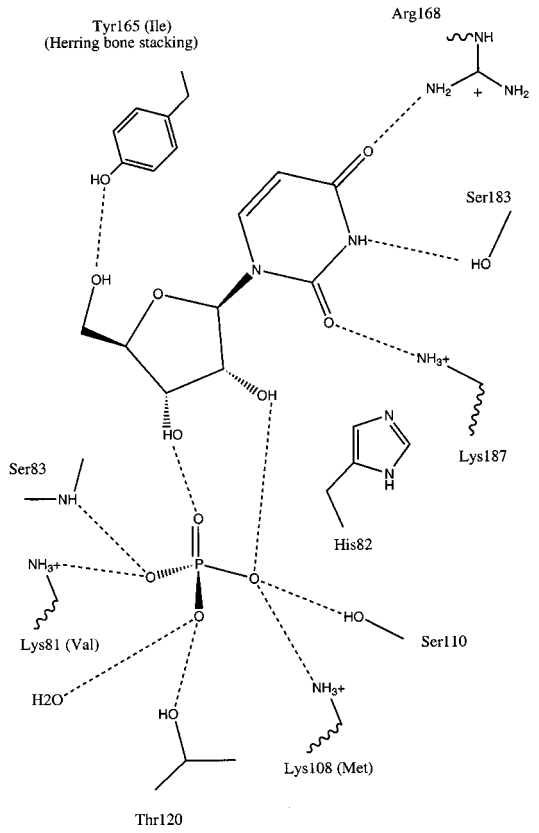

Figure 12 Active-site residues in the PyNP structure in a closed-cleft conformation

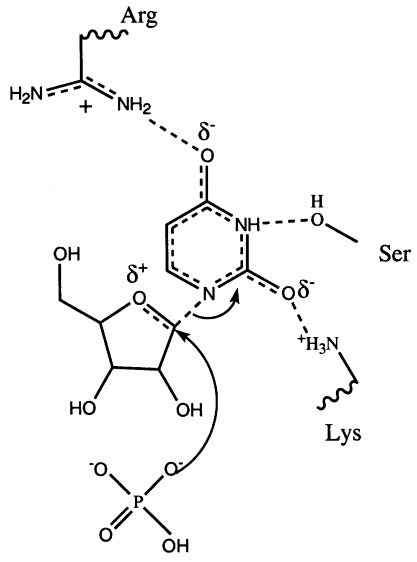

Figure 13 Proposed catalytic mechanism for the NP-II family, analogous to that of the NP-I family

sites in the structures of *E. coli* TP and *B. stearothermophilus* PyNP suggests one possible explanation for this difference. In both *E. coli* and human TP, which are reported to be specific for the 2′-deoxyribose moiety, a methionine residue replaces Lys-108 of PyNP. This substitution may create a different hydrogen-bonding scheme with the phosphate oxygen that binds to the 2′-hydroxy group of the ribose moiety, and may account for the difference in substrate specificity [117]. The crystal structure of PyNP in a closed conformation also suggests that the pyrimidine nucleoside binds in a high-energy conformation with a glycosidic torsion angle that is classified as +*antiperiplanar* and an unusual C4′-endo pucker of the sugar ring. A similar high-energy conformation was noted previously in the PNP structures of the NP-I family. The overall orientations of the nucleoside and phosphate ion are also very similar to those observed in the structures of the NP-I family.

Although the catalytic mechanism for the NP-II family has not been studied to the same extent as for PNP, it is likely that the mechanism is very similar in nature to that proposed for hPNP. A proposed mechanism for the NP-II family is shown schematically in Figure 13. The steps of this mechanism are analogous to those discussed above for the NP-I family, and begin with weakening of the glycosidic bond due to the high-energy conformation of the bound pyrimidine nucleoside. The glycosidic bond is weakened further as electrons flow from O-4′ of the ribose moiety (where an oxocarbenium ion is subsequently formed) to the pyrimidine ring, and are stabilized through interactions with the positively charged lysine and arginine residues. The phosphate ion, which binds on the α-side of the ribose ring, is then positioned to attack the C-1′ position of the ribose ring to yield α-ribose 1-phosphate and the free pyrimidine base. The role of His-82, which is absolutely conserved in the NP-II family (see Figures 13 and 14), in the mechanism is not known, but it could potentially be involved in stabilizing the transition state, or donating a proton to the C-1 position of the pyrimidine ring following glycosidic cleavage.

NP-II SEQUENCE ANALYSIS

Members of the NP-II family show a high degree of sequence similarity: all the known sequences share between 33% and 67% identity, and thus are expected to have similar structures. The similarity in sequences of enzymes belonging to the NP-II family is shown in Figure 14. Residues in the α-domain are more highly conserved than residues in the α/β-domain. Use of standard searching methods has revealed a possible relationship with the sequence of AnPRT, which has also been noted in a motif study involving sequences from both PNPs and PyNPs [88]. AnPRT catalyses the second step in tryptophan biosynthesis, in which phosphoribosylanthranilate and pyrophosphate are formed from anthranilate and phosphoribosyl pyrophosphate [26]. AnPRT from *Hafnia alvei* is reported to function as a homodimer with a molecular mass of 70 kDa [133]. The N-terminal regions of NP-II sequences and AnPRT show the most significant similarity. A motif study in our laboratory [86] has also shown AnPRT sequences to share significant similarities with the phosphate-binding region in NP-II sequences. The similarities between PyNP and AnPRT, including the reactions catalysed, the properties of the reactants and products, the amino acid sequences and the quaternary structures, suggest a possible structural relationship between these two enzymes. AnPRT has been crystallized previously [133], and a preliminary description of the structure has recently been reported [134]. That study confirmed that AnPRT is homologous with members of the NP-II family, and distinctly different from any other previously reported phosphoribosyltransferase structures [135–142].

NP-II INHIBITOR DESIGN

Inhibiting TP is of therapeutic interest for several reasons. Inhibition of the nucleoside salvage pathway may be an effective

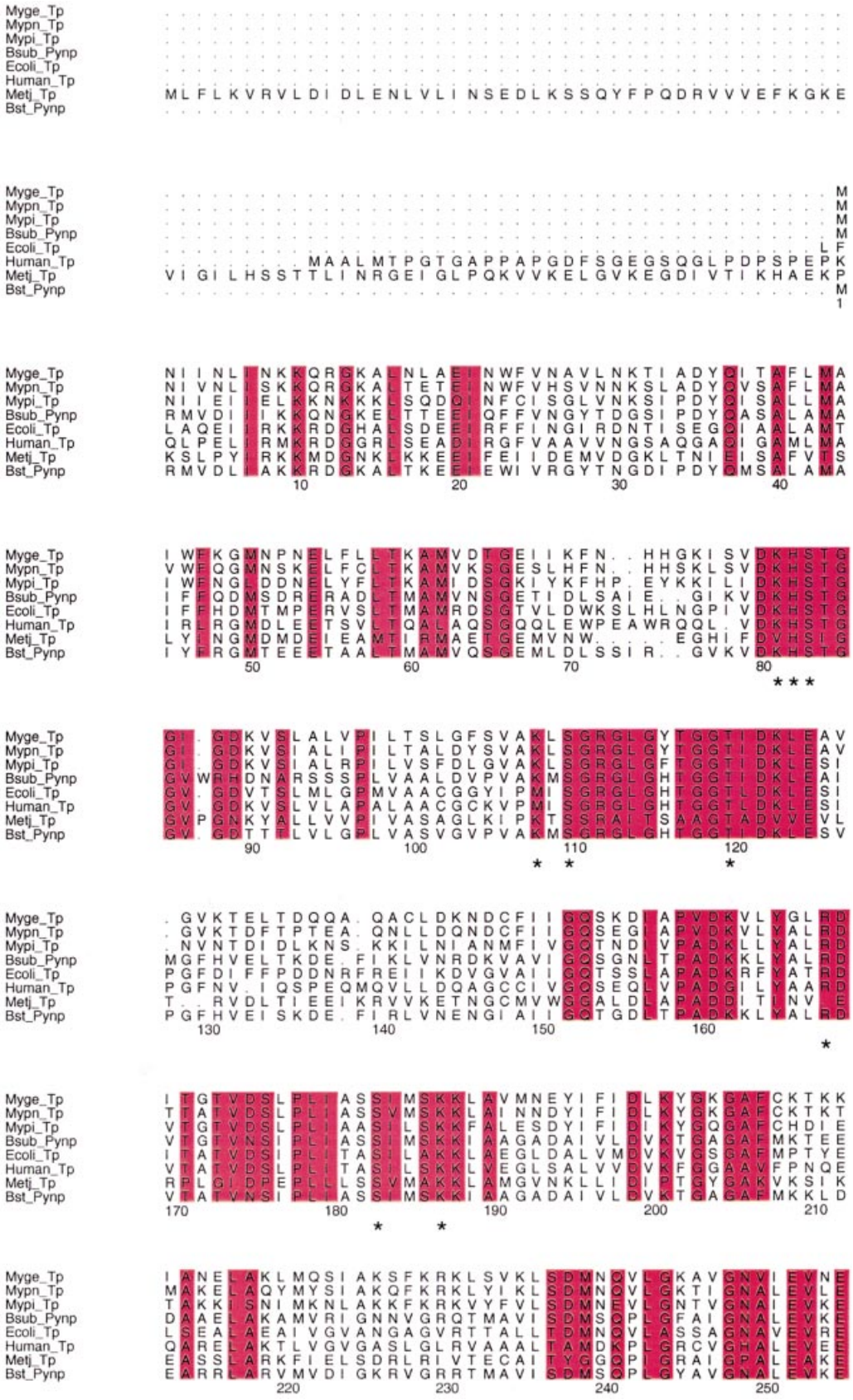

Figure 14 For legend see opposite

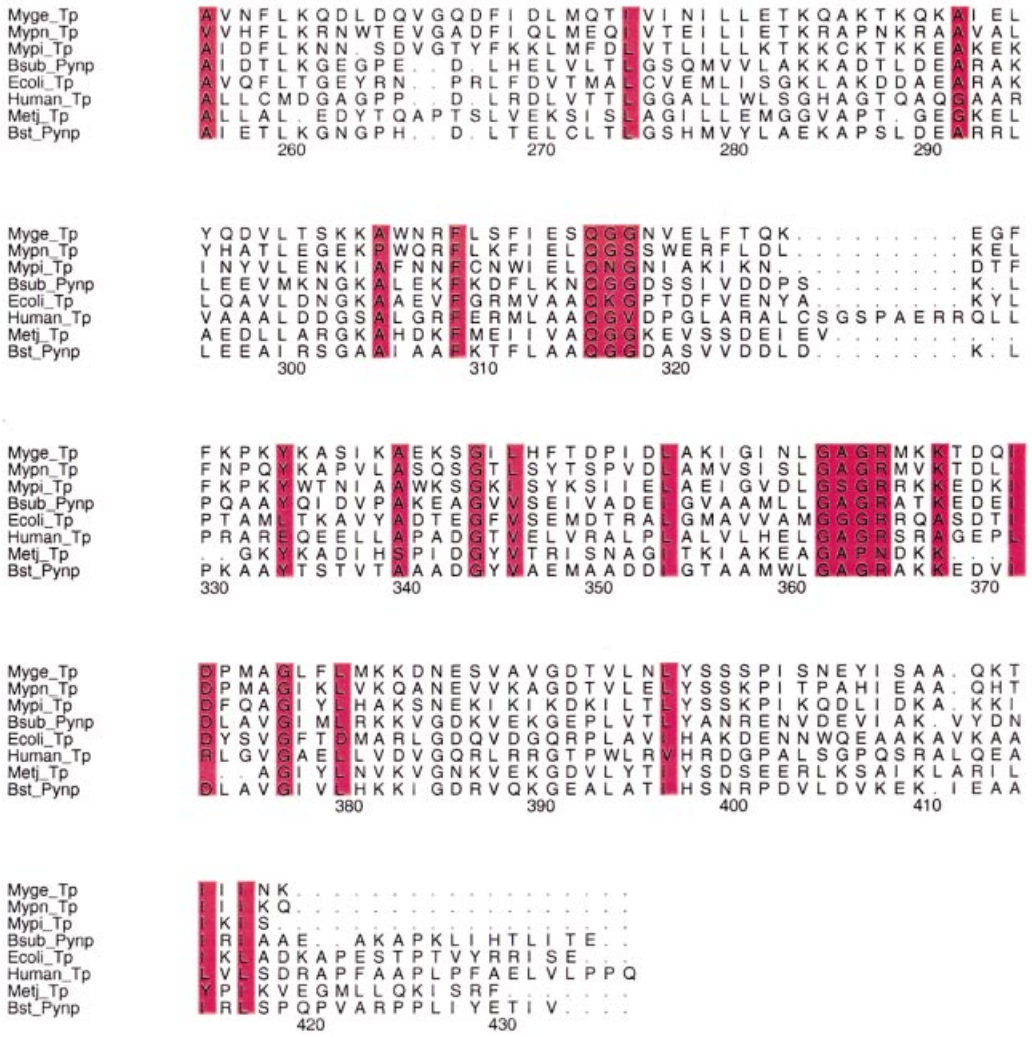

Figure 14 Multiple sequence alignment of members of the NP-II family

Myge_Tp, *Mycoplasma genitalium* TP; Mypn_Tp, *Mycoplasma pneumoniae* TP; Mypi_Tp, *Mycoplasma pirum* TP; Bsub_Pynp, *Bacillus subtilis* PyNP; Ecoli_Tp, *Escherichia coli* TP; Human_Tp, human TP/platelet-derived endothelial cell growth factor; Metj_Tp, *Methanococcus jannashii* TP; Bst_Pynp, *Bacillus stearothermophilus* PyNP. The numbering refers to the *Bacillus stearothermophilus* PyNP sequence. Highly conserved regions have been coloured red, and active-site residues are indicated by *. This Figure was prepared using ALSCRIPT [164].

chemotherapeutic strategy in cancer, since some tumour cells depend heavily on this pathway for their proliferation [143,144]. In addition, various fluoropyrimidines have been used widely as chemotherapeutic agents; the catalytic action of TP on the glycosidic bond of these pyrimidine analogues is thought to be a key step in their activation and regulation [145–148]. Inhibitors may therefore be useful in modulating these reactions in both the synthetic and phosphorolytic directions, as well as with regard to the ribosyltransferase activity. Gene therapy has been suggested as a means of providing tissue-directed expression of TP [149]. It has furthermore been shown that specific thymidine concentrations, administered concurrently with various fluoropyrimidines, can be cytotoxic to several tumour cell lines [150–152]. Thus being able to control thymidine levels *in vivo* may be useful in various chemotherapeutic strategies. The recent discovery that TP also functions as an angiogenic growth factor and is found in abnormally high levels in several tumour cell lines draws even more attention to this enzyme as a drug target in cancer treatment.

Most inhibitors of TP are pyrimidine or pyrimidine nucleoside analogues. Several early studies reported on the binding properties of 1-substituted uracil rings [153], 5- and 6-substituted uracil rings [154], 1-substituted uracil rings with the addition of various hydrophobic substituents at the 5- and 6-positions [155], and 5′-substituents of thymidine, as well as various other substitutions on the ribose ring [156]. A later study by Baker and Kelley [157] reported on 80 different uracil compounds with hydrophobic substituents at the 1-, 5- or 6-positions. These compounds were tested for binding affinity for TP from both rabbit liver and *E. coli*. The most effective inhibitors from this study were those containing a 2,4-dimethylanilino, phenethylamino or phenylbutylamino substituent at the 6-position, which had IC_{50} values that ranged from 53 to 110 μM for TP from rabbit liver. Studies of pyrimidine acyclonucleosides showed acyclothymidine [5-methyl-1-(2′-hydroxyethoxymethyl)uracil] to be an effective inhibitor of UP (K_i 3 μM), but it did not inhibit TP [158]. A more recent study, however, suggests that acyclothymidine may be an effective inhibitor of both UP and TP [159]. This suggestion

resulted from studying the inhibition of the phosphorolysis of 5′-deoxy-5-fluorouridine in intestinal homogenates from human, rabbit, rat and mouse. Acyclothymidine was shown to be the most potent inhibitor among a group of several acyclopyrimidine nucleosides, with a K_i (measured against the intestinal tissue homogenate, which contained both TP and UP) of 0.36 mM in human, 0.94 mM in rabbit, 0.0097 mM in rat and 0.0176 mM in mouse. Niedzwicki and co-workers [160] also reported a study of 87 pyrimidine base or nucleoside analogues as potential inhibitors of both TP and UP, which resulted in the development of structure–activity relationships that are useful in the rational design of more potent inhibitors. That study showed 5-bromouracil to be the most potent inhibitor of TP, with a K_i of 33 μM, and 5-benzyloxybenzylacyclouridine to be the most potent inhibitor of UP, with a K_i of 0.17 μM [160]. A study [161] that used the structure of *E. coli* TP to rationally design a series of 5-substituted 6-aminouracils and 7-substituted pyrrolo[2,3-*d*]-pyrimidine-2,4-diones resulted in the synthesis of several compounds that were tested for inhibition of human placental TP. The most effective inhibitors were 7-(2-aminomethyl)-pyrrolo[2,3-*d*]pyrimidine-2,4-dione (IC_{50} 44.0 μM), 5-bromo-6-aminouracil (IC_{50} 7.6 μM) and 5-cyano-6-[3-(methylamino)-propyl]uracil (IC_{50} 3.8 μM). The limited success in developing effective TP inhibitors and in formulating accurate structure–activity relationships may be due, in part, to the lack of a detailed structural model from the NP-II family in its active closed conformation. Our recent structural studies of PyNP provide a model for the closed conformation, and may prove valuable to the structure-based drug design efforts to produce potent inhibitors.

CONCLUDING REMARKS

The NP-I and NP-II families represent two structurally distinct families of enzymes that catalyse the same fundamental biochemical reaction. These families represent the only two folds known to be involved in the phosphorolysis of a wide range of purine and pyrimidine nucleosides. Analysis of the sequences of members of the NP-I family in combination with the known three-dimensional structures has revealed regions of the NP-I fold that may account for the differences in substrate specificity and in quaternary structure among family members. Detailed structural analyses have provided significant information concerning the structure–function relationships in both of these families, and help to explain the differences and similarities that exist among their respective members. While the folds of the NP-I and NP-II families are not related, the arrangement of substrates in the active sites and the conformation of the bound nucleosides show striking similarities. In addition, although the catalytic mechanism of TP has not been studied to the extent of that of PNP, it is likely to be very similar to that proposed for the NP-I family. The NP-I and NP-II families provide a clear example of two distinct enzyme families that show similar substrate specificity and probably employ a similar catalytic mechanism while also maintaining distinct three-dimensional folds. Despite the similarity of the reactions catalysed in these two families, the uniqueness of their respective folds suggests that they have evolved independently. Information concerning structure–function relationships in these families suggests possible evolutionary pathways, and is also valuable as the search for clinically useful inhibitors continues.

REFERENCES

1 Levene, P. A. (1906) Autolysis. Harvey Lect. **1**, 89
2 Levene, P. A. and Medigreceanu, F. (1911) On nucleases. J. Biol. Chem. **9**, 65–83
3 Levene, P. A., Yamagawa, M. and Weber, I. (1924) On nucleosidases. I. General Properties. J. Biol. Chem. **60**, 693–706
4 Levene, P. A. and Weber, I. (1924) On nucleosidases. II. Purification of the enzyme. J. Biol. Chem. **60**, 707–720
5 Deutsch, W. and Laser, R. (1930) Experimentelle studien über den nucleinstoffwechsel. XIX. Mitteilung. Zur kenntnis der nucleosidase. Verhalten einer nucleosidase aus rinderknochenmark zu einem splatprodukt der thymusnucleinsäure. Z. Physiol. Chem. **186**, 1–10
6 Klein, W. (1935) Experimentelle studien über den nucleinstoffwechsel. XXXVII. Über nucleosidase. Z. Physiol. Chem. **231**, 125–148
7 Kalckar, H. M. (1945) Enzymatic synthesis of a nucleoside. J. Biol. Chem. **158**, 723–724
8 Kalckar, H. (1945) Enzymatic synthesis of nucleosides. Fed. Proc. Fed. Am. Soc. Exp. Biol. **4**, 248–252
9 Kalckar, H. (1947) The enzymatic synthesis of purine ribosides. J. Biol. Chem. **167**, 477–486
10 Friedkin, M. and Roberts, D. (1954) The enzymatic synthesis of nucleosides. I. Thymidine phosphorylase in mammalian tissue. J. Biol. Chem. **207**, 245–256
11 Friedkin, M. and Roberts, D. (1954) The enzymatic synthesis of nucleosides. II. Thymidine and related pyrimidine nucleosides. J. Biol. Chem. **207**, 257–266
12 Paege, L. M. and Schlenk, F. (1952) Bacterial uracil riboside phosphorylase. Arch. Biochem. Biophys. **40**, 42–49
13 Gopaul, D. N., Meyer, S. L., Degano, M., Sacchettini, J. C. and Schramm, V. L. (1996) Inosine-uridine nucleoside hydrolase from *Crithidia fasciculata*. Genetic characterization, crystallization, and identification of histidine 241 as a catalytic site residue. Biochemistry **35**, 5963–5970
14 Carter, C. E. (1951) Partial purification of a non-phosphorylytic uridine nucleosidase from yeast. J. Am. Chem. Soc. **73**, 1508–1510
15 Duerre, J. A. (1962) A hydrolytic nucleosidase acting on *S*-adenosylhomocysteine and on 5′-methylthioadenosine. J. Biol. Chem. **237**, 3737–3741
16 Hurwitz, J., Heppel, L. A. and Horecker, B. L. (1957) The enzymatic cleavage of adenylic acid to adenine and ribose 5-phosphate. J. Biol. Chem. **226**, 525–540
17 Ueda, K., Fukushima, M., Okayama, H. and Hayaishi, O. (1975) Nicotinamide adenine dinucleotide glycohydrolase from rat liver nuclei. Isolation and characterization of a new enzyme. J. Biol. Chem. **250**, 7541–7546
18 Smith, E. L., Kimmel, J. R., Brown, D. M. and Thompson, E. O. P. (1955) Isolation and properties of a crystalline mercury derivative of a lysozyme from papaya latex. J. Biol. Chem. **215**, 67–89
19 Conchie, J., Findlay, J. and Levvy, G. A. (1959) Mammalian glycosidases. Distribution in the body. Biochem. J. **71**, 318–325
20 Gottschalk, A. (1960) Neuraminidase. Enzymes 2nd Ed. **4**, 461–473
21 Short, S. A., Armstrong, S. R., Ealick, S. E. and Porter, D. J. (1996) Active site amino acids that participate in the catalytic mechanism of nucleoside 2′-deoxyribosyltransferase. J. Biol. Chem. **271**, 4978–4987
22 Smar, M., Short, S. A. and Wolfenden, R. (1991) Lyase activity of nucleoside 2-deoxyribosyltransferase: transient generation of ribal and its use in the synthesis of 2′-deoxynucleosides. Biochemistry **30**, 7908–7912
23 Flaks, J. G., Erwin, M. J. and Buchanan, J. M. (1957) Biosynthesis of the purines. XVI. The synthesis of adenosine 5′-phosphate and 5-amino-4-imidazolecarboxamide ribotide by a nucleotide pyrophosphorylase. J. Biol. Chem. **228**, 201–213
24 Olsen, A. S. and Milman, G. (1974) Chinese hamster hypoxanthine-guanine phosphoribosyltransferase. Purification, structural, and catalytic properties. J. Biol. Chem. **249**, 4030–4037
25 Imsande, J. and Handler, P. (1961) Biosynthesis of diphosphopyridine nucleotide. III. Nicotinic acid mononucleotide pyrophosphorylase. J. Biol. Chem. **236**, 525–530
26 Crawford, I. P. (1989) Evolution of a biosynthetic pathway: the tryptophan paradigm. Annu. Rev. Microbiol. **43**, 567–600
27 Neuhard, J. (1983) Utilization of preformed pyrimidine bases and nucleosides. In Metabolism of Nucleotides, Nucleosides, and Nucleobases in Microorganisms (Munch-Peterson, A., ed.), pp. 95–148, Academic Press, London
28 Nygaard, P. (1983) Utilization of preformed purine bases and nucleosides. In Metabolism of Nucleotides, Nucleosides, and Nucleobases in Microorganisms (Munch-Peterson, A., ed.), pp. 27–93, Academic Press, London
29 Imada, A. and Igarasi, S. (1967) Ribosyl and deoxyribosyl transfer by bacterial enzyme systems. J. Bacteriol. **94**, 1551–1559
30 Stoeckler, J. D. (1984) Purine nucleoside phosphorylase: a target for chemotherapy. In Development in Cancer Chemotherapy (Glazer, R. E., ed.), pp. 35–60, CRC Press, Boca Raton, FL
31 Giblett, E. R., Ammann, A. J., Wara, D. W., Sandman, R. and Diamond, L. K. (1975) Nucleoside-phosphorylase deficiency in a child with severely defective T-cell immunity and normal B-cell immunity. Lancet **i**, 1010–1013
32 Ealick, S. E., Babu, Y. S., Bugg, C. E., Erion, M. D., Guida, W. C., Montgomery, J. A. and Secrist, III, J. A. (1991) Application of crystallographic and modeling methods in the design of purine nucleoside phosphorylase inhibitors. Proc. Natl. Acad. Sci. U.S.A. **88**, 11540–11544

33 Miyazono, K., Okabe, T., Urabe, A., Takaku, F. and Heldin, C. H. (1987) Purification and properties of an endothelial cell growth factor from human platelets. J. Biol. Chem. **262**, 4098–4103

34 Sorscher, E. J., Peng, S., Bebok, Z., Allan, P. W., Bennett, Jr, L. L. and Parker, W. B. (1994) Tumor cell bystander killing in colonic carcinoma utilizing the *Escherichia coli* DeoD gene to generate toxic purines. Gene Ther. **1**, 233–228

35 Secrist, III, J. A., Parker, W. B., Allan, P. W., Bennett, Jr, L. L., Waud, W. R., Truss, J. W., Fowler, A. T., Montgomery, J. A., Ealick, S. E., Wells, A. H. et al. (1999) Gene therapy of cancer: activation of nucleoside prodrugs with *E. coli* purine nucleoside phosphorylase. Nucleosides Nucleotides **18**, 745–757

36 Bzowska, A., Kulikowska, E. and Shugar, D. (1990) Properties of purine nucleoside phosphorylase (PNP) of mammalian and bacterial origin. Z. Naturforsch. C **45**, 59–70

37 Kalckar, H. M. (1947) Differential spectrophotometry of purine compounds by means of specific enzymes. III. Studies of the enzymes of purine metabolism. J. Biol. Chem. **167**, 461–475

38 Kim, B. K., Cha, S. and Parks, R. E. (1968) Purine nucleoside phosphorylase from human erythrocytes. I. Purification and properties. J. Biol. Chem. **243**, 1763–1770

39 Lewis, A. S. and Glantz, M. D. (1976) Bovine brain purine-nucleoside phosphorylase purification, characterization, and catalytic mechanism. Biochemistry **15**, 4451–4457

40 Lewis, A. S. and Glantz, M. D. (1976) Monomeric purine nucleoside phosphorylase from rabbit liver. Purification and characterization. J. Biol. Chem. **251**, 407–413

41 Price, V. E., Otey, M. C. and Plesner, P. (1955) Preparation of nucleoside phosphorylase from calf spleen. Methods Enzymol. **2**, 448–453

42 Milman, G., Anton, D. L. and Weber, J. L. (1976) Chinese hamster purine-nucleoside phosphorylase: purification, structural, and catalytic properties. Biochemistry **15**, 4967–4973

43 Jensen, K. F. and Nygaard, P. (1975) Purine nucleoside phosphorylase from *Escherichia coli* and *Salmonella typhimurium*. Purification and some properties. Eur. J. Biochem. **51**, 253–265

44 Cacciapuoti, G., Porcelli, M., Bertoldo, C., De Rosa, M. and Zappia, V. (1994) Purification and characterization of extremely thermophilic and thermostable 5′-methylthioadenosine phosphorylase from the archaeon *Sulfolobus solfataricus*. Purine nucleoside phosphorylase activity and evidence for intersubunit disulfide bonds. J. Biol. Chem. **269**, 24762–24769

45 Shirea, H. and Yokozeki, K. (1991) Purification and properties of orotidine-phosphorolyzing enzyme and purine nucleoside phosphorylase from *Erwinia carotovora*. Agric. Biol. Chem. **55**, 1849–1857

46 Gilpin, R. W. and Sadoff, H. L. (1971) Physical and catalytic properties of the purine nucleoside phosphorylases from cells and spores of *Bacillus cereus* T. J. Biol. Chem. **246**, 1475–1480

47 Seeger, C., Poulsen, C. and Dandanell, G. (1995) Identification and characterization of genes (xapA, xapB, and xapR) involved in xanthosine catabolism in *Escherichia coli*. J. Bacteriol. **177**, 5506–5516

48 Senesi, S., Falcone, G., Mura, U., Sgarrella, F. and Ipata, P. L. (1976) A specific adenosine phosphorylase, distinct from purine nucleoside phosphorylase. FEBS Lett. **64**, 353–357

49 Hori, N., Watanabe, M., Yamazaki, Y. and Nmikami, Y. (1989) Purification and characterization of a second thermostable purine nucleoside phosphorylase in *Bacillus stearothermophilus* JTS 859. Agric. Biol. **53**, 3219–3224

50 Krenitsky, T. A., Mellors, J. W. and Barclay, R. K. (1965) Pyrimidine nucleosidases: their classification and relationship to uric acid ribonucleoside phosphorylase. J. Biol. Chem. **240**, 1281–1286

51 Krenitsky, T. A., Barclay, M. and Jacquez, J. A. (1964) Specificity of mouse uridine phosphorylase. Chromatography, purification, and properties. J. Biol. Chem. **239**, 805–812

52 Krenitsky, T. A. (1976) Uridine phosphorylase from *Escherichia coli*. Kinetic properties and mechanism. Biochim. Biophys. Acta **429**, 352–358

53 McIvor, R. S., Wohlhueter, R. M. and Plagemann, P. G. (1983) Uridine phosphorylase from *Acholeplasma laidlawii*: purification and kinetic properties. J. Bacteriol. **156**, 198–204

54 Watanabe, S. and Uchica, T. (1995) Cloning and expression of human uridine phosphorylase. Biochem. Biophys. Res. Commun. **216**, 265–272

55 Della Ragione, F., Oliva, A., Gragnaniello, V., Russo, G. L., Palumbo, R. and Zappia, V. (1990) Physicochemical and immunological studies on mammalian 5′-deoxy-5′-methylthioadenosine phosphorylase. J. Biol. Chem. **265**, 6241–6246

56 Ferro, A. J., Wrobel, N. C. and Nicolette, J. A. (1979) 5-Methylthioribose 1-phosphate: a product of partially purified, rat liver 5′-methylthioadenosine phosphorylase activity. Biochim. Biophys. Acta **570**, 65–73

57 Friedkin, M. (1950) Desoxyribose-1-phosphate. II. The isolation of crystalline desoxyribose-1-phosphate. J. Biol. Chem. **184**, 449–459

58 Kim, B. K., Cha, S. and Parks, Jr, R. E. (1968) Purine nucleoside phosphorylase from human erythroyctes. II. Kinetic analysis and substrate-binding studies. J. Biol. Chem. **243**, 1771–1776

59 Krenitsky, T. (1967) Purine nucleoside phosphorylase: kinetics, mechanism, and specificity. Mol. Pharmacol. **3**, 526–536

60 Carlson, J. D. and Fischer, A. G. (1979) Characterization of the active site of homogeneous thyroid purine nucleoside phosphorylase. Biochim. Biophys. Acta **571**, 21–34

61 Lewis, A. S. and Lowy, B. A. (1979) Human erythrocyte purine nucleoside phosphorylase: molecular weight and physical properties. A Theorell-Chance catalytic mechanism. J. Biol. Chem. **254**, 9927–9932

62 Porter, D. J. (1992) Purine nucleoside phosphorylase. Kinetic mechanism of the enzyme from calf spleen. J. Biol. Chem. **267**, 7342–7351

63 Erion, M. D., Takabayashi, K., Smith, H. B., Kessi, J., Wagner, S., Honger, S., Shames, S. L. and Ealick, S. E. (1997) Purine nucleoside phosphorylase. 1. Structure-function studies. Biochemistry **36**, 11725–11734

64 Erion, M. D., Stoeckler, J. D., Guida, W. C., Walter, R. L. and Ealick, S. E. (1997) Purine nucleoside phosphorylase. 2. Catalytic mechanism. Biochemistry **36**, 11735–11748

65 Stoeckler, J. D., Poirot, A. F., Smith, R. M., Parks, Jr, R. E., Ealick, S. E., Takabayashi, K. and Erion, M. D. (1997) Purine nucleoside phosphorylase. 3. Reversal of purine base specificity by site-directed mutagenesis. Biochemistry **36**, 11749–11756

66 Fedorov, A., Shi, W., Kicska, G., Fedorov, E., Tyler, P. C., Furneaux, R. H., Hanson, J. C., Gainsford, G. J., Larese, J. Z., Schramm, V. L. and Almo, S. C. (2001) Transition state structure of purine nucleoside phosphorylase and principles of atomic motion in enzymatic catalysis. Biochemistry **40**, 853–860

67 Tebbe, J., Bzowska, A., Wielgus-Kutrowska, B., Schroder, W., Kazimierczuk, Z., Shugar, D., Saenger, W. and Koellner, G. (1999) Crystal structure of the purine nucleoside phosphorylase (PNP) from *Cellulomonas* sp. and its implication for the mechanism of trimeric PNPs. J. Mol. Biol. **294**, 1239–1255

68 Kraut, A. and Yamada, E. W. (1971) Cytoplasmic uridine phosphorylase of rat liver. Characterization and kinetics. J. Biol. Chem. **246**, 2021–2030

69 Zappia, V., Della Ragione, F., Pontoni, G., Gragnaniello, V. and Carteni-Farina, M. (1988) Human 5′-deoxy-5′-methylthioadenosine phosphorylase: kinetic studies and catalytic mechanism. Adv. Exp. Med. Biol. **250**, 165–177

70 Garbers, D. L. (1978) Demonstration of 5′-methylthioadenosine phosphorylase activity in various rat tissues. Some properties of the enzyme from rat lung. Biochim. Biophys. Acta **523**, 82–93

71 Shugart, L., Mahoney, L. and Chastain, B. (1981) Kinetic studies of *Drosophila melanogaster* methylthioadenosine nucleoside phosphorylase. Int. J. Biochem. **13**, 559–564

72 Ealick, S. E., Rule, S. A., Carter, D. C., Greenhough, T. J., Babu, Y. S., Cook, W. J., Habash, J., Helliwell, J. R., Stoeckler, J. D. and Bugg, C. E. (1990) Three-dimensional structure of human erythrocytic purine nucleoside phosphorylase at 3.2 Å resolution. J. Biol. Chem. **265**, 1812–1820

73 Narayana, S. V. L., Bugg, C. E. and Ealick, S. E. (1997) Refined structure of purine nucleoside phosphorylase at 2.75 Å resolution. Acta Crystallogr. D **53**, 131–142

74 Bzowska, A., Luic, M., Schroder, W., Shugar, D., Saenger, W. and Koellner, G. (1995) Calf spleen purine nucleoside phosphorylase: purification, sequence and crystal structure of its complex with an N(7)-acycloguanosine inhibitor. FEBS Lett. **367**, 214–218

75 Koellner, G., Luic, M., Shugar, D., Saenger, W. and Bzowska, A. (1997) Crystal structure of calf spleen purine nucleoside phosphorylase in a complex with hypoxanthine at 2.15 Å resolution. J. Mol. Biol. **265**, 202–216

76 Mao, C., Cook, W. J., Zhou, M., Federov, A. A., Almo, S. C. and Ealick, S. E. (1998) Calf spleen purine nucleoside phosphorylase complexed with substrates and substrate analogues. Biochemistry **37**, 7135–7146

77 Luic, M., Koellner, G., Shugar, D., Saenger, W. and Bzowska, A. (2001) Calf spleen purine nucleoside phosphorylase: structure of its ternary complex with an N(7)-acycloguanosine inhibitor and a phosphate anion. Acta Crystallogr. D **57**, 30–36

78 Shi, W., Basso, L. A., Santos, D. S., Tyler, P. C., Furneaux, R. H., Blanchard, J. S., Almo, S. C. and Schramm, V. L. (2001) Structures of purine nucleoside phosphorylase from *Mycobacterium tuberculosis* in complexes with immucillin-H and its pieces. Biochemistry **40**, 8204–8215

79 Appleby, T. C., Erion, M. D. and Ealick, S. E. (1999) The structure of human 5′-deoxy-5′-methylthioadenosine phosphorylase at 1.7 Å resolution provides insights into substrate binding and catalysis. Structure **7**, 629–641

80 Mao, C., Cook, W. J., Zhou, M., Koszalka, G. W., Krenitsky, T. A. and Ealick, S. E. (1997) The crystal structure of *Escherichia coli* purine nucleoside phosphorylase: A comparison with the human enzyme reveals a conserved topology. Structure **5**, 1373–1383

81 Koellner, G., Luic, M., Shugar, D., Saenger, W. and Bzowska, A. (1998) Crystal structure of the ternary complex of *E. coli* purine nucleoside phosphorylase with formycin B, a structural analogue of the substrate inosine, and phosphate (sulphate) at 2.1 Å resolution. J. Mol. Biol. **280**, 153–166

82 Zhao, B. (1991) Three-dimensional structure of uridine phosphorylase from *Escherichia coli* at 3.0 Å resolution, Doctoral Dissertation, University of Alabama-Birmingham, Birmingham, AL

83 Morgunova, E. Y., Mikhailov, A. M., Popov, A. N., Blagova, E. V., Smirnova, E. A., Vainshtein, B. K., Mao, C., Armstrong, S. R., Ealick, S. E., Komissarov, A. A. et al. (1995) Atomic structure at 2.5 Å resolution of uridine phosphorylase from *E. coli* as refined in the monoclinic crystal lattice. FEBS Lett. **367**, 183–187

84 Appleby, T. C., Mathews, I. I., Porcelli, M., Cacciapuoti, G. and Ealick, S. E. (2001) Three-dimensional structure of a hyperthermophilic 5′-deoxy-5′-methylthioadenosine phosphorylase from *Sulfolobus solfataricus*. J. Biol. Chem. **276**, 39232–39242

85 Altschul, S. F., Gish, W., Miller, W., Myers, E. W. and Lipman, D. J. (1990) Basic local alignment search tool. J. Mol. Biol. **215**, 403–410

86 Pugmire, M. J. (1999) Structural studies of purine nucleoside phosphorylase and pyrimidine nucleoside phosphorylase. Doctoral Dissertation, Cornell University, Ithaca, NY

87 Grundy, W. N., Bailey, T. L. and Elkan, C. P. (1996) ParaMEME: a parallel implementation and a web interface for a DNA and protein motif discovery tool. Comput. Appl. Biosci. **12**, 303–310

88 Mushegian, A. R. and Koonin, E. V. (1994) Unexpected sequence similarity between nucleosidases and phosphoribosyltransferases of different specificity. Protein Sci. **3**, 1081–1088

89 Zappia, V., Oliva, A., Cacciapuoti, G., Galletti, P., Mignucci, G. and Carteni-Farina, M. (1978) Substrate specificity of 5′-methylthioadenosine phosphorylase from human prostate. Biochem. J. **175**, 1043–1050

90 Lee, J. E., Cornell, K. A., Riscoe, M. K. and Howell, P. L. (2001) Structure of *E. coli* 5′-methylthioadenosine/S-adenosylhomocysteine nucleosidase reveals similarity to the purine nucleoside phosphorylases. Structure **9**, 941–953

91 Bennett, Jr, L. L., Allan, P. W., Noker, P. E., Rose, L. M., Niwas, S., Montgomery, J. A. and Erion, M. D. (1993) Purine nucleoside phosphorylase inhibitors: biochemical and pharmacological studies with 9-benzyl-9-deazaguanine and related compounds. J. Pharmacol. Exp. Ther. **266**, 707–714

92 Stoeckler, J. D., Cambor, C. and Parks, Jr, R. E. (1980) Human erythrocytic purine nucleoside phosphorylase: reaction with sugar-modified nucleoside substrates. Biochemistry **19**, 102–107

93 Rich, K. C., Arnold, W. J., Palella, T. and Fox, I. H. (1979) Cellular immune deficiency with autoimmune hemolytic anemia in purine nucleoside phosphorylase deficiency. Am. J. Med. **67**, 172–176

94 Stoop, J. W., Zegers, B. J., Hendrickx, G. F., van Heukelom, L. H., Staal, G. E., de Bree, P. K., Wadman, S. K. and Ballieux, R. E. (1977) Purine nucleoside phosphorylase deficiency associated with selective cellular immunodeficiency. N. Engl. J. Med. **296**, 651–655

95 Tuttle, J. V. and Krenitsky, T. A. (1984) Effects of acyclovir and its metabolites on purine nucleoside phosphorylase. J. Biol. Chem. **259**, 4065–4069

96 Krenitsky, T. A., Tuttle, J. V., Miller, W. H., Moorman, A. R., Orr, G. F. and Beauchamp, L. (1990) Nucleotide analogue inhibitors of purine nucleoside phosphorylase. J. Biol. Chem. **265**, 3066–3069

97 Nakamura, C. E., Chu, S. H., Stoeckler, J. D. and Parks, Jr, R. E. (1986) Inhibition of purine nucleoside phosphorylase by 9-(phosphonoalkyl)hypoxanthines. Biochem. Pharmacol. **35**, 133–136

98 Montgomery, J. A. (1993) Purine nucleoside phosphorylase: a target for drug design. Med. Res. Rev. **13**, 209–228

99 Montgomery, J. A., Niwas, S., Rose, J. D., Secrist, III, J. A., Babu, Y. S., Bugg, C. E., Erion, M. D., Guida, W. C. and Ealick, S. E. (1993) Structure-based design of inhibitors of purine nucleoside phosphorylase: I. 9-(arylmethyl) derivatives of 9-deazaguanine. J. Med. Chem. **36**, 55–69

100 Secrist, III, J. A., Niwas, S., Rose, J. D., Babu, Y. S., Bugg, C. E., Erion, M. D., Guida, W. C., Ealick, S. E. and Montgomery, J. A. (1993) Structure-based design of inhibitors of purine nucleoside phosphorylase. 2. 9-Alicyclic and 9-heteroalicyclic derivatives of 9-deazaguanine. J. Med. Chem. **36**, 1847–1854

101 Erion, M. D., Niwas, S., Rose, J. D., Ananthan, S., Allen, M., Secrist, III, J. A., Babu, Y. S., Bugg, C. E., Guida, W. C., Ealick, S. E. et al. (1993) Structure-based design of inhibitors of purine nucleoside phosphorylase. 3. 9-Arylmethyl derivatives of 9-deazaguanine substituted on the methylene group. J. Med. Chem. **36**, 3771–3783

101a Erratum (1994) J. Med. Chem. **37**, 1034

102 Guida, W. C., Elliott, R. D., Thomas, H. J., Secrist, III, J. A., Babu, Y. S., Bugg, C. E., Erion, M. D., Ealick, S. E. and Montgomery, J. A. (1994) Structure-based design of inhibitors of purine nucleoside phosphorylase. 4. A study of phosphate mimics. J. Med. Chem. **37**, 1109–1114

103 Kelley, J. L., McLean, E. W., Crouch, R. C., Averett, D. R. and Tuttle, J. V. (1995) [[(Guaninylalkyl)phosphinico]methyl]phosphonic acids. Multisubstrate analogue inhibitors of human erythrocyte purine nucleoside phosphorylase. J. Med. Chem. **38**, 1005–1014

104 Miles, R. W., Tyler, P. C., Furneaux, R. H., Bagdassarian, C. K. and Schramm, V. L. (1998) One-third-the-sites transition-state inhibitors for purine nucleoside phosphorylase. Biochemistry **37**, 8615–8621

105 Laster, L. and Blair, A. (1963) An intestinal phosphorylase for uric acid ribonucleoside. J. Biol. Chem. **238**, 3348–3357

106 Zimmerman, M. and Seidenberg, J. (1964) Deoxyribosyl transfer. I. Thymidine phosphorylase and nucleoside deoxyribosyltransferase in normal and malignant tissues. J. Biol. Chem. **239**, 2618–2621

107 Zimmerman, M. and Seidenberg, J. (1964) Deoxyribosyl transfer. II. Nucleoside: pyrimidine deoxyribosyltransferase activity of three partially purified thymidine phosphorylases. J. Biol. Chem. **239**, 2622–2627

108 Gallo, R. C. and Breitman, T. R. (1968) The enzymatic mechanisms for deoxythymidine synthesis in human leukocytes. II. Comparison of deoxyribosyl donors. J. Biol. Chem. **243**, 4936–4942

109 Schwartz, M. (1971) Thymidine phosphorylase from *Escherichia coli*. Properties and kinetics. Eur. J. Biochem. **21**, 191–198

110 Avraham, Y., Grossowicz, N. and Yashphe, J. (1990) Purification and characterization of uridine and thymidine phosphorylase from *Lactobacillus casei*. Biochim. Biophys. Acta **1040**, 287–293

111 Desgranges, C., Razaka, G., Rabaud, M. and Bricaud, H. (1981) Catabolism of thymidine in human blood platelets: purification and properties of thymidine phosphorylase. Biochim. Biophys. Acta **654**, 211–218

112 Cook, W. J., Koszalka, G. W., Hall, W. W., Burns, C. L. and Ealick, S. E. (1987) Crystallization and preliminary x-ray investigation of thymidine phosphorylase from *Escherichia coli*. J. Biol. Chem. **262**, 3788–3789

113 Yamada, E. W. (1968) Pyrimidine nucleoside phosphorylases of rat liver. Separation by ion exchange chromatography and studies of the effect of cytidine or uridine administration. J. Biol. Chem. **243**, 1649–1655

114 Razzell, W. E. and Khorana, H. G. (1958) Purification and properties of a pyrimidine deoxyriboside phosphorylase from *Escherichia coli*. Biochim. Biophys. Acta **28**, 562–566

115 Hamamoto, T., Noguchi, T. and Midorikawa, Y. (1996) Purification and characterization of purine nucleoside phosphorylase and pyrimidine nucleoside phosphorylase from *Bacillus stearothermophilus* TH 6-2. Biosci. Biotechnol. Biochem. **60**, 1179–1180

116 Scocca, J. J. (1971) Purification and substrate specificity of pyrimidine nucleoside phosphorylase from *Haemophilus influenzae*. J. Biol. Chem. **246**, 6606–6610

117 Pugmire, M. J. and Ealick, S. E. (1998) The crystal structure of pyrimidine nucleoside phosphorylase in a closed conformation. Structure **6**, 1467–1479

118 Pugmire, M. J., Cook, W. J., Jasanoff, A., Walter, M. R. and Ealick, S. E. (1998) Structural and theoretical studies suggest domain movement produces an active conformation of thymidine phosphorylase. J. Mol. Biol. **281**, 285–299

119 Walter, M. R., Cook, W. J., Cole, L. B., Short, S. A., Koszalka, G. W., Krenitsky, T. A. and Ealick, S. E. (1990) Three-dimensional structure of thymidine phosphorylase from *Escherichia coli* at 2.8 Å resolution. J. Biol. Chem. **265**, 14016–14022

120 Krenitsky, T. A. (1968) Pentosyl transfer mechanisms of the mammalian nucleoside phosphorylases. J. Biol. Chem. **243**, 2871–2875

121 Krenitsky, T. A. and Tuttle, J. V. (1982) Correlation of substrate-stabilization patterns with proposed mechanisms for three nucleoside phosphorylases. Biochim. Biophys. Acta **703**, 247–249

122 Iltzsch, M. H., el Kouni, M. H. and Cha, S. (1985) Kinetic studies of thymidine phosphorylase from mouse liver. Biochemistry **24**, 6799–6807

123 Hammer-Jespersen, K., Munch-Petersen, A., Schwartz, M. and Nygaard, P. (1971) Induction of enzymes involved in the catabolism of deoxyribonucleosides and ribonucleosides in *Escherichia coli* K12. Eur. J. Biochem. **19**, 533–538

124 Schwartz, E. L., Hoffman, M., O'Connor, C. J. and Wadler, S. (1992) Stimulation of 5-fluorouracil metabolic activation by interferon-α in human colon carcinoma cells. Biochem. Biophys. Res. Commun. **182**, 1232–1239

125 Takebayashi, Y., Yamada, K., Ohmoto, Y., Sameshima, T., Miyadera, K., Yamada, Y., Akiyama, S. and Aikou, T. (1995) The correlation of thymidine phosphorylase activity with the expression of interleukin 1 alpha, interferon alpha and interferon gamma in human colorectal carcinoma. Cancer Lett. **95**, 57–62

126 Miyadera, K., Dohmae, N., Takio, K., Sumizawa, T., Haraguchi, M., Furukawa, T., Yamada, Y. and Akiyama, S. (1995) Structural characterization of thymidine phosphorylase purified from human placenta. Biochem. Biophys. Res. Commun. **212**, 1040–1045

127 Asai, K., Hirano, T., Kaneko, S., Moriyama, A., Nakanishi, K., Isobe, I., Eksioglu, Y. Z. and Kato, T. (1992) A novel glial growth inhibitory factor, gliostatin, derived from neurofibroma. J. Neurochem. **59**, 307–317

128 Fox, S. B., Westwood, M., Moghaddam, A., Comley, M., Turley, H., Whitehouse, R. M., Bicknell, R., Gatter, K. C. and Harris, A. L. (1996) The angiogenic factor platelet-derived endothelial cell growth factor/thymidine phosphorylase is up-regulated in breast cancer epithelium and endothelium. Br. J. Cancer **73**, 275–280

129 Maehara, Y., Sakaguchi, Y., Kusumoto, T., Kusumoto, H. and Sugimachi, K. (1989) Species differences in substrate specificity of pyrimidine nucleoside phosphorylase. J. Surg. Oncol. **42**, 184–186

130 Takebayashi, Y., Yamada, K., Maruyama, I., Fujii, R., Akiyama, S. and Aikou, T. (1995) The expression of thymidine phosphorylase and thrombomodulin in human colorectal carcinomas. Cancer Lett. **92**, 1–7

131 Toi, M., Hoshina, S., Taniguchi, T., Yamamoto, Y., Ishitsuka, H. and Tominaga, T. (1995) Expression of platelet-derived endothelial cell growth factor/thymidine phosphorylase in human breast cancer. Int. J. Cancer **64**, 79–82

132 Yoshimura, A., Kuwazuru, Y., Furukawa, T., Yoshida, H., Yamada, K. and Akiyama, S. (1990) Purification and tissue distribution of human thymidine phosphorylase; high expression in lymphocytes, reticulocytes and tumors. Biochim. Biophys. Acta **1034**, 107–113

133 Edwards, S. L., Kraut, J., Xuong, N., Ashford, V., Halloran, T. P. and Mills, S. E. (1988) Crystallization and purification of the enzyme anthranilate phosphoribosyl transferase. J. Mol. Biol. **203**, 523–524

134 Mayans, O., Ivens, A., Kirschner, K. and Wilmanns, M. (2000) Completion of the tryptophan biosynthesis pathway: problematic MAD on TrpD. American Crystallographic Association Meeting, St. Paul, MN, 22–27 July 2000, Collected Abstracts vol. 45, p. 45, American Crystallographic Association, Buffalo

135 Phillips, C. L., Ullman, B., Brennan, R. G. and Hill, C. P. (1999) Crystal structures of adenine phosphoribosyltransferase from *Leishmania donovani*. EMBO J. **18**, 3533–3545

136 Cheong, C. G., Escalante-Semerena, J. C. and Rayment, I. (1999) The three-dimensional structures of nicotinate mononucleotide:5,6-dimethylbenzimidazole phosphoribosyltransferase (CobT) from *Salmonella typhimurium* complexed with 5,6-dimethybenzimidazole and its reaction products determined to 1.9 Å resolution. Biochemistry **38**, 16125–16135

137 Sharma, V., Grubmeyer, C. and Sacchettini, J. C. (1998) Crystal structure of quinolinic acid phosphoribosyltransferase from *Mycobacterium tuberculosis*: a potential TB drug target. Structure **6**, 1587–1599

138 Schumacher, M. A., Carter, D., Scott, D. M., Roos, D. S., Ullman, B. and Brennan, R. G. (1998) Crystal structures of *Toxoplasma gondii* uracil phosphoribosyltransferase reveal the atomic basis of pyrimidine discrimination and prodrug binding. EMBO J. **17**, 3219–3232

139 Vos, S., de Jersey, J. and Martin, J. L. (1997) Crystal structure of *Escherichia coli* xanthine phosphoribosyltransferase. Biochemistry **36**, 4125–4134

140 Eads, J. C., Ozturk, D., Wexler, T. B., Grubmeyer, C. and Sacchettini, J. C. (1997) A new function for a common fold: the crystal structure of quinolinic acid phosphoribosyltransferase. Structure **5**, 47–58

141 Scapin, G., Grubmeyer, C. and Sacchettini, J. C. (1994) Crystal structure of orotate phosphoribosyltransferase. Biochemistry **33**, 1287–1294

142 Eads, J. C., Scapin, G., Xu, Y., Grubmeyer, C. and Sacchettini, J. C. (1994) The crystal structure of human hypoxanthine-guanine phosphoribosyltransferase with bound GMP. Cell **78**, 325–334

143 Niedzwicki, J. G., Chu, S. H., el Kouni, M. H., Rowe, E. C. and Cha, S. (1982) 5-Benzylacyclouridine and 5-benzyloxybenzylacyclouridine, potent inhibitors of uridine phosphorylase. Biochem. Pharmacol. **31**, 1857–1861

144 Schwartz, P. M. and Milstone, L. M. (1988) Thymidine phosphorylase in human epidermal keratinocytes. Biochem. Pharmacol. **37**, 353–355

145 Birnie, G. D., Kroeger, H. and Heidelberger, C. (1962) Studies of fluorinated pyrimidines. XVIII. The degradation of 5-fluoro-2′-deoxy-uridine and related compounds by nucleoside phophorylase. Biochemistry **3**, 566–572

146 Schwartz, E. L., Baptiste, N., Megati, S., Wadler, S. and Otter, B. A. (1995) 5-Ethoxy-2′-deoxyuridine, a novel substrate for thymidine phosphorylase, potentiates the antitumor activity of 5-fluorouracil when used in combination with interferon, an inducer of thymidine phosphorylase expression. Cancer Res. **55**, 3543–3550

147 Schwartz, E. L., Baptiste, N., Wadler, S. and Makower, D. (1995) Thymidine phosphorylase mediates the sensitivity of human colon carcinoma cells to 5-fluorouracil. J. Biol. Chem. **270**, 19073–19077

148 Woodman, P. W., Sarrif, A. M. and Heidelberger, C. (1980) Specificity of pyrimidine nucleoside phosphorylases and the phosphorolysis of 5-fluoro-2′-deoxyuridine. Cancer Res. **40**, 507–511

149 Patterson, A. V., Zhang, H., Moghaddam, A., Bicknell, R., Talbot, D. C., Stratford, I. J. and Harris, A. L. (1995) Increased sensitivity to the prodrug 5′-deoxy-5-fluorouridine and modulation of 5-fluoro-2′-deoxyuridine sensitivity in MCF-7 cells transfected with thymidine phosphorylase. Br. J. Cancer **72**, 669–675

150 Kirkwood, J. M., Ensminger, W., Rosowsky, A., Papathanasopoulos, N. and Frei, III, E. (1980) Comparison of pharmacokinetics of 5-fluorouracil and 5-fluorouracil with concurrent thymidine infusions in a Phase I trial. Cancer Res. **40**, 107–113

151 Lee, S. S., Giovanella, B. C., Stehlin, Jr, J. S. and Brunn, J. C. (1979) Regression of human tumors established in nude mice after continuous infusion of thymidine. Cancer Res. **39**, 2928–2933

152 Reiter, H. (1979) Effect of thymidine on the survival of mice with EL4 tumors. Cancer Res. **39**, 4856–4860

153 Baker, B. R. and Kawazu, M. (1967) Irreversible enzyme inhibitors. LXXVI. Inhibitors of thymidine phosphorylase. II. Hydrophobic bonding by 1-substituted uracils. J. Med. Chem. **10**, 302–304

154 Baker, B. R. and Kawazu, M. (1967) Irreversible enzyme inhibitors. LXXVIII. Inhibitors of thymidine phosphorylase. IV. Hydrophobic bonding by uracils substituted at the 5 and 6 positions. J. Med. Chem. **10**, 311–313

155 Baker, B. R., Kawazu, M., Santi, D. V. and Schwan, T. J. (1967) Irreversible enzyme inhibitors. LXXVII. Inhibitors of thymidine phosphorylase. III. Hydrophobic bonding by 1-substituted uracils containing additional substituents at the 5 and 6 positions. J. Med. Chem. **10**, 304–311

156 Baker, B. R. (1967) Irreversible enzyme inhibitors. LXXV. Inhibitors of thymidine phosphorylase. I. Mode of ribofuranose binding. J. Med. Chem. **10**, 297–301

157 Baker, B. R. and Kelley, J. L. (1971) Irreversible enzyme inhibitors. 188. Inhibition of mammalian thymidine phosphorylase. J. Med. Chem. **14**, 812–816

158 Niedzwicki, J. G., el Kouni, M. H., Chu, S. H. and Cha, S. (1981) Pyrimidine acyclonucleosides, inhibitors of uridine phosphorylase. Biochem. Pharmacol. **30**, 2097–2101

159 Hamada, A., Fukushima, S., Saneyoshi, M., Kawaguchi, T. and Nakano, M. (1995) Inhibition of 5′-deoxy-5-fluorouridine phosphorolysis by acyclopyrimidine nucleosides in intestinal tissue homogenates. Biol. Pharm. Bull. **18**, 172–175

160 Niedzwicki, J. G., el Kouni, M. H., Chu, S. H. and Cha, S. (1983) Structure-activity relationship of ligands of the pyrimidine nucleoside phosphorylases. Biochem. Pharmacol. **32**, 399–415

161 Hirota, K., Sawada, M., Sajiki, H. and Sako, M. (1997) Synthesis of 6-aminouracils and pyrrolo[2,3-d]pyrimidine-2,4-diones and their inhibitory effect on thymidine phosphorylase. Nucleic Acids Symp. Ser. **37**, 59–60

162 Kraulis, P. J. (1991) MOLSCRIPT: a program to produce both detailed and schematic plots of protein structures. J. Appl. Crystallogr. **24**, 946–950

163 Carson, M. (1987) Ribbons models of macromolecules. J. Mol. Graphics **5**, 103–106

164 Barton, G. J. (1993) ALSCRIPT: a tool to format multiple sequence alignments. Protein Eng. **6**, 37–40